2D VOLUMETRIC STRAIN IMAGING THROUGH THZ TIME-DOMAIN SPECTROSCOPY OF STRONTIUM TITANATE FLEXIBLE COMPOSITE ACTING AS REMOTE PASSIVE SENSOR

by

Luis Miguel Reig Buades

A Thesis

Submitted to the Faculty of Purdue University

In Partial Fulfillment of the Requirements for the degree of

Master of Science in Aeronautics and Astronautics

School of Aeronautics and Astronautics

West Lafayette, Indiana

December 2020

THE PURDUE UNIVERSITY GRADUATE SCHOOL
STATEMENT OF COMMITTEE APPROVAL

Dr. Vikas Tomar, Chair

School of Aeronautics and Astronautics

Dr. Wenbin Yu

School of Aeronautics and Astronautics

Dr. Alexey Shashurin

Department of Agricultural Economics

Approved by:

Dr. Gregory A. Blaisdell

ACKNOWLEDGMENTS

I would like to pay special regards to my supervisor Prof. Vikas Tomar for his support and mentorship during the development of this research. Your insightful feedback has pushed me to sharpen my thinking and has brought my work to a higher level.

I would also like to thank the team of the Inter-facial Multi-Physics Lab for their collaboration, with special thanks to Abhijeet Dhiman and Ayush Rai for their valuable help and guidance.

In addition, I would like to thank my parents for their wise counseling and sympathetic understanding throughout all my life that has been crucial to reach my academic goals.

TABLE OF CONTENTS

LIST OF FIGURES

LIST OF ABBREVIATIONS

THz TDS:	Terahertz Time-Domain Spectroscopy
EMP:	Electromagnetic Pulse
STO:	Strontium Titanate
ToA:	Time of Arrival
DIC:	Digital Image Correlation
SAW:	Surface Acoustic Wave
IDT:	Inter-Digital Transducer

LIST OF SYMBOLS

ε_r: Dielectric permittivity

v_w: Propagation speed of electromagnetic wave in dielectric media

c: Speed of light in vacuum

n: Index of refraction

μ_r: Magnetic permeability

d: inter-planar spacing

λ: wavelength

k: positive integer

e_{vol}: 2D Volumetric Strain

C: Calibration Constant

ΔToA: Increase in Time of Arrival

ToA: Time of Arrival

d_{anten}: distance between antennas

$v_{w,air}$: wave speed propagation in air

$v_{w,sensor}$: wave speed propagation through senor

t_{sensor}: sensor thickness

χ_v: magnetic susceptibility

$\varepsilon_{r,eff}$: effective dielectric permittivity of sensor

ε_p: dielectric permittivity of particle

ε_m: dielectric permittivity of matrix

v_r: volumetric ratio of particles in composite

b: fitting Constant

t_f: thickness of deformed composite

t_o: initial thickness of composite

e_{zz}: transversal strain

e_{xx}: planar strain in x direction

e_{yy}: planar strain in y direction

v: Poisson's ratio

α: Linear direct proportionality

$1/\alpha$: Linear inverse Proportionality

$\boldsymbol{\varepsilon_{\xi\xi}}$: dielectric permittivity of composite in principal direction $\xi\xi$

$\boldsymbol{\varepsilon^0}$: dielectric permittivity of vacuum

$\boldsymbol{\varepsilon^i}$: dielectric permittivity of undeformed composite

$\boldsymbol{\varepsilon_m}$: dielectric permittivity of matrix

$\boldsymbol{\sigma_p}$: stress in particle

$\boldsymbol{\sigma_m}$: stress in matrix

$\boldsymbol{E_m}$: Modulus of elasticity of matrix

$\boldsymbol{\phi}$: Phase-Delay

$\vec{\boldsymbol{a}}$: sampled amplitude of unloaded wave data expressed as vector

$\vec{\boldsymbol{b}}$: s ampled amplitude of loaded wave data expressed as vector

ABSTRACT

Strain field imaging can have important applications in the fields of material characterization and structural health monitoring. In the former, this analysis is used for the experimental assessment of mechanical behavioral laws; and in the latter, it is applied for damage prediction purposes in many industries where good structural maintenance increases the safety and productivity of operations. Terahertz Time-Domain Spectroscopy (THz TDS) is a relatively new technique capable of measuring the amplitude and phase of an electromagnetic pulse (EMP) in the THz band, which is characterized by very low absorbance in most dielectric materials and allows to study small variations in a material's electromagnetic properties.

The following thesis defends how applying a composite of Strontium Titanate (STO) particles dispersed in a low dielectric matrix to a structural component, a material that changes its dielectric constant when loaded, and sensing the change in dielectric properties of the coating at different loadings, a new non-destructive and remote sensing method of strain field mapping can be achieved. This method has made possible to correlate strain to changes in the time of arrival (TOA) of the EMP, and then use this correlation to measure the localized strain fields through previous material-specific calibration.

The following thesis contains a deep literature review of current state of the art methods for strain field mapping such as Holography or Digital Image Correlation (DIC) and how these relate to strain sensing through THz TDS spectroscopy in terms of advantages and disadvantages. Other methods of sensing strain with THz TDS are also reviewed.

Afterwards, a theoretical analysis of our strain sensing method is performed, attending to all the physical factors in the passive sensor that affect THz TDS readings when strained and therefore explaining the physics in which our sensor is based. A mathematical model is also produced that allows to study how different material parameters will affect the sensitivity of the composite.

Finally, strain mappings of different geometries that produce strain concentrations are obtained through THz TDS and compared with FEA and DIC to show the current capabilities of the method, together with a discussion of the results and setting the basis for future work.

THESIS ORGANIZATION

This thesis is paper based, the first two chapters consist of introducing the reader to the basics of the work carried out, while stating the problem that this research tries to solve and the motivation to solve it. Then, the manuscript where this work is to be published is included as the third chapter, and the conclusions are performed in the 4th and final chapter.

Chapter 1 consists of the introduction to the research; in this section the objective of this thesis is clearly stated together with the possible outcomes and applications of achieving it. In summary, it is to produce a 2D volumetric strain imaging technique through a passive sensor, which could have applications in structural health monitoring and validation of material studies.

Chapter 2 is a literature review where the technique to be developed is compared to others already available in the literature, highlighting its advantages and disadvantages and therefore understanding its potential applications.

Chapter 3 consists of the manuscript in which this research is to be published. Firstly, it develops a theoretical modeling where the physics involved in this sensing procedure are detailed and mathematically modeled. Then, it explains the experimental methodology carried out to prove the functioning of the novel strain imaging method. It also contains the results of this thesis, where different geometries that produce localized strain gradients are mapped with this technique and shown, together with a critical discussion.

Finally, chapter 4 states the conclusions, where a critical assessment is performed of the outcome of this work and the background for future work is established.

CHAPTER 1. INTRODUCTION

1.1 Statement of the problem and motivation

Terahertz Time-Domain Spectroscopy (THz TDS) is increasingly becoming a highly valued technique with a wide range of applications that go all the way from engineering disciplines, to medicine and security. It basically consists of analyzing how an electromagnetic wave in the THz gap changes as it goes through different media by comparing a wave that has passed through the media to be studied to one that passes simply through air, which allows for material characterization, chemical studies, and determination of dielectric properties [1]. Since the THz region encompasses the far infrared region between 0.1 and 10 THz, it makes possible a far better resolution than other micro-wave methods, which together with its ability to go through most dielectric materials makes for a new non-destructive stress analysis approach with high potential in remote sensing applications.

The following study analyses how the application of a coating with high dielectrostriction, meaning that its dielectric properties vary with strain, to a structural component could produce a passive sensor for the measurement of strain fields. This coating is composed of Strontium Titanate particles (STO) in a low dielectric flexible matrix; by dispersing STO, a high dielectric material that is already dielectrostrictive by itself, in a polymer with low dielectric constant, a flexible composite is obtained with high dielectrostriction coefficient. . When probed through THz TDS, changes in the arrival time of a THz pulse that goes through it can be measured and correlated to strain because of its dielectric behavior. By taking advantage of the high resolution of electromagnetic waves in the THz spectra and their capacity to go through a wide range of materials, this approach makes possible to measure the strain state of components even when there are opaque materials in the THz wave path, as long as they are transparent to THz waves, which

includes most polymers and ceramics. Therefore, producing a novel contactless structural health monitoring approach that also allows for sensing of components inaccessible through other non-destructive methods if they are obstructed by opaque media.

This method could prove better than the optical methods that are currently used to measure strain fields because THz waves are able to penetrate through many opaque materials, which would allow to study components unreachable by radiation in the optical frequency.

1.2 THz Time-Domain Spectroscopy Fundamentals

THz TDS is a strong spectroscopic technique that allows to study the properties of matter through probing with a short pulse of radiation in the THz frequency range. The THz frequency range is usually defined as containing the electromagnetic waves with frequencies between 100 GHz and 10 THz.

THz radiation proposes several useful advantages for spectroscopic purposes. Together with its high resolution and beam-like properties, most non-conductive materials are transparent to them, meaning it will act like X-rays, but it also has the benefit that it is a non-ionizing radiation, so it does not require any personal protection arrangements. Also, many important materials have spectral fingerprints to THz radiation, which allows to use it for identification in security applications such as explosives[2] and narcotics[3] detection, or medical applications[4] to identify chemical components or even cancer. It also allows for measurement of conductive properties[5] without needing any electronic attachment, with important uses in the electronic industry and for material science since it can quantify phase transitions[6].

A THz TDS spectroscopy system usually consists of a femtosecond laser that is split into two beams, which are referred to as pump beam and probe beam. The former is used to generate the THz radiation and the latter is used to measure the time at which a given amplitude is measured.

The THz radiation is generated and detected through so-called photoconductive antennas. The emitter antenna produces the THz radiation when it is excited through the pump beam pulse; on the other side, the receptor antenna measures the amplitude of the electromagnetic field it is receiving at the moment it is strobed by the probe beam pulse. The time at which the receptor measures the amplitude it is sensing can be modified by changing the length that probe laser through a moving mirror, called a variable delay. This way, it is possible to map the whole amplitude in time of the THz pulse. **Figure 1** shows a schematic of the THz TDS set up used in this research.

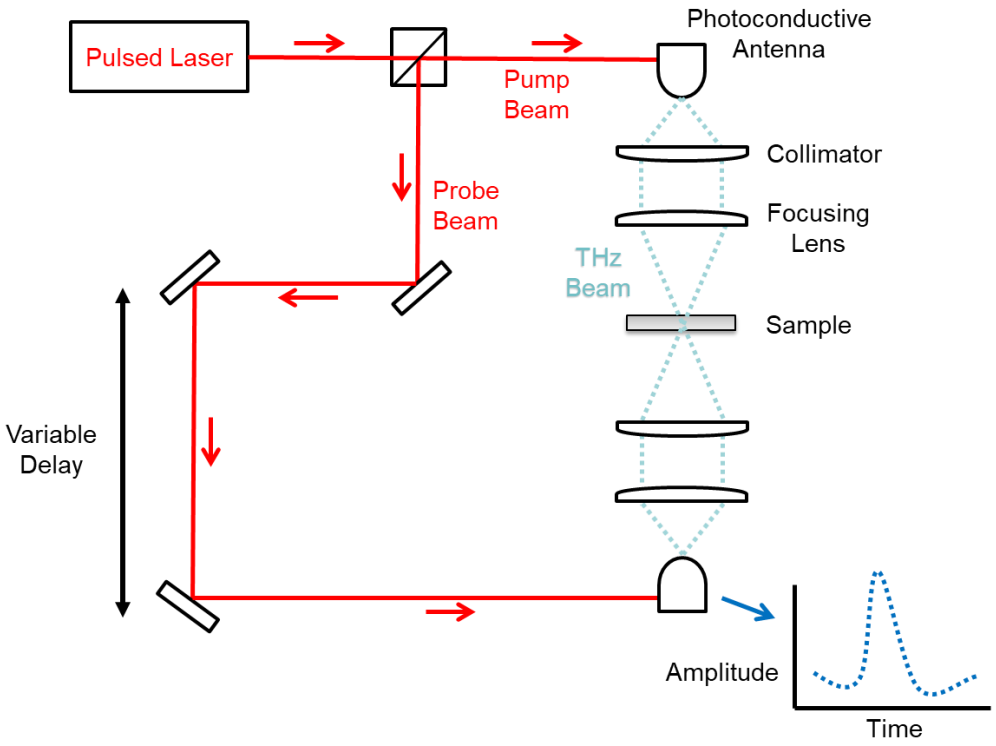

Figure 1: Schematic of THz TDS set-up showing how a laser is split into a pump beam for radiation generation and a probe beam to measure radiation amplitude at each time through a variable delay. Not all THz set-ups include focusing lenses, which are only required for spectroscopy of small regions.

In order to adequate the THz radiation for the measurements, collimators and focusing lenses are applied to the in the antennas. The collimator will apply the same direction to all the emitted THz waves and the focusing lenses will focus the THz beam in a small region to increase the resolution to around 0.4 mm in the focus point, whose value is set by the wavelength of waves with THz frequency. It must be mentioned that not all THz set-ups use focusing lenses, which are only required for high-resolution applications such as imaging. There are some laboratories working in increasing the resolution of THz waves beyond wave-length resolution, Ref. [7] produced THz measurements with a resolution 0.02 mm using a laser filament, although these procedures are not usually applied to the widely available systems at the moment.

THz measurements are usually classified in reflection or transmission configurations depending on whether the THz wave is reflected on a metallic surface before reaching the receptor antenna, this can be understood looking at **Figure 2**. The current study has been carried out using a transmission configuration in which only the composite has been stretched and studied without applying it to any structural component. If it was to be attached to a component, theoretically the coating will experience the same strain state as the surface of that component, so all the theoretical assessments in the current thesis should apply to the measurements. The differences will be that in transmission measurements the deformation of the component will affect THz readings, so the calibration will be required to include both the component and the composite; while in the reflection measurements the wave will only probe the sensor, going two times through it, which should increase sensitivity and will only require calibration of the sensor without the component affecting the readings. It must be noted that reflection measurements are usually harder to prepare since the correct alignment of the antennas is more intricate.

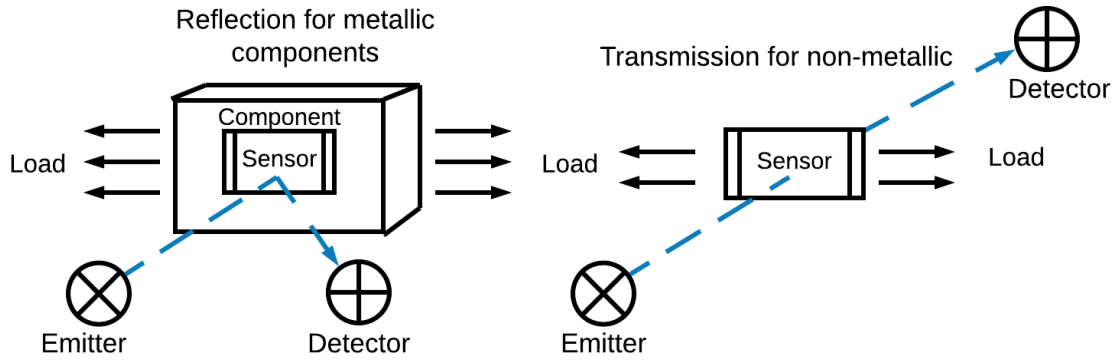

Figure 2: Representation of transmission and reflection THz measurements. Reflection measurements are based on the THz wave being reflected from a metallic surface before reaching the receptor.

1.3 Strain Measurement with THz TDS of passive sensor attachment

The following subsection provides a brief introduction of the theory behind how the sensor will affect the THz wave when strained and therefore the basis of our sensing procedure. This serves as a theoretical background to understand the statements made in the literature review, but the theory is further developed in the theoretical model section, which includes a more detailed mathematical model.

An electromagnetic wave propagates through a medium with velocity v_w, which depends on the index of refraction n of that media. The index of refraction of a material can be considered directly proportional to the square root of its relative dielectric constant ε_r and magnetic permeability μ_r, and therefore the wave speed through a material of a THz wave can be related to the speed of light c through **Eq. (1)**. Non-doped strontium titanate is diamagnetic at room temperature[8], meaning that it has a constant magnetic permeability with a value a few thousands below unity, and therefore it suffers a very small magnetic repulsion when a magnetic field is applied. Regarding dielectric behavior of the composite, Strontium titanate is a paraelectric

material at ambient temperature[9] and the elastomer polymers that will be used can be considered dielectric, meaning that the polarization of both components in the composite is recovered when the electromagnetic field acting on it stops. This lack of ferromagnetic and ferroelectric properties makes Strontium Titanate ideal for this purpose, since it is one of the few Perovskites with high dielectric constant that has this desirable behavior of no electromagnetic memory.

$$v_w = \frac{c}{n} = \frac{c}{\sqrt{\varepsilon_r \, \mu_r}} \simeq \frac{c}{\sqrt{\varepsilon_r}} \qquad \textbf{(1)}$$

This implies that changes in the dielectric properties of the coating will produce a change in the wave speed of the THz pulse going through it, varying the arrival time of the THz wave, which we can measure; this change in arrival time should recover when the specimen is unloaded due the composite's dielectric properties previously explained, which makes this process applicable to structural health monitoring. If the distances that the pulse is traveling through each media were known together with their dielectric properties, the arrival time of the wave to the receptor could be calculated analytically by applying simple kinematics. This principle can be understood looking at **Figure 3**.

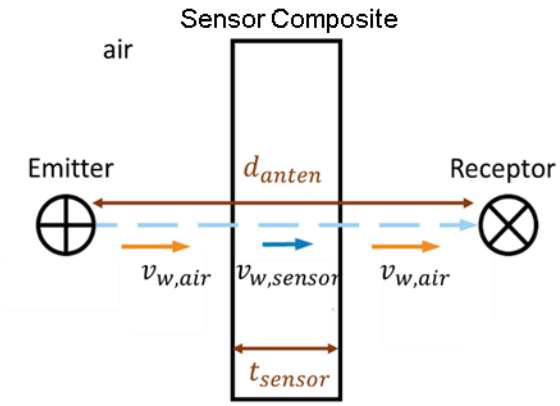

Figure 3: Visualization of the variables that kinematically are going to affect the time of arrival of the THz wave to the receptor in a transmission configuration. If all these variables were known, the wave time of arrival could be analytically calculated through kinematics.

Induced by the previously explained property of electromagnetic waves, when the component is loaded in this study, there are 3 parameters affecting the measurements and changing the time of arrival of the THz wave by changes in the media through which the wave travels, which are shown schematically in **Figure 4**. Studying them for the case of a tensile load. The first is the composite changing size when the tensile load is applied by means of the Poisson's effect, this will be independent of coating application since it is too thin to be affected, and it will not mean a change in dielectric through the component, but it will mean a smaller time for the wave to have the lower speed corresponding to that material index of refraction. Then, regarding the coating, applying a load will produce two effects; on one hand, an in-plane deformation of the composite will pull particles closer or further apart, changing the number of high dielectric particles in the THz beam [10]; on the other hand, Strontium Titanate is a material that suffers an important change in the dielectric constant when stressed [11], [12]; both of this effects will decrease the index of refraction of the coating, making the wave pass faster though it.

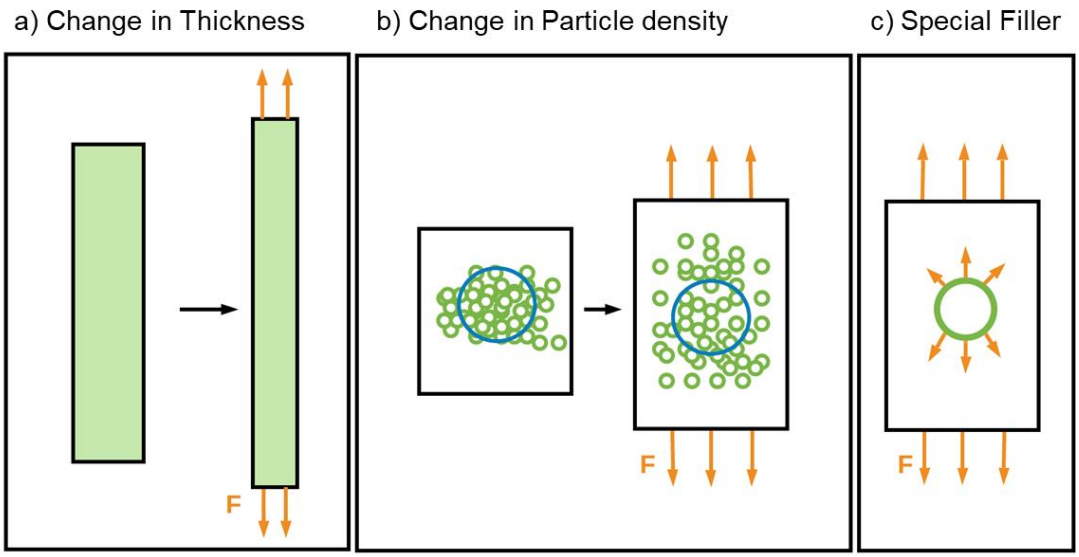

Figure 4: Mechanisms affecting the electromagnetic wave arrival time from the emitter to the receptor, green circles represent strontium titanate particles a) Component getting thinner due to the tensile load, decreasing the distance through which the wave is slower when traveling the material b) Stretching the composite coating, separating the dielectric particles and decreasing index of refraction c) Loading the composite will produce a stress in the strontium titanate particles inside it, which decreases their dielectric constant.

From this information, it can be extracted that the sensor will make the wave reach faster when stretched and therefore decrease its ToA, and the opposite will happen when compressed, which allows us to measure strain through previous calibration. Furthermore, this helps to understand the different objectives we are looking for in the sensor design. Regarding the change in thickness, we are trying to obtain a composite material with the highest dielectric constant possible, such that when its thickness changes, it affects more the ToA. Furthermore, the sensor design will also aim to obtain the highest dielectrostriction attainable, and all of this attending the high elastic recovery needed for a strain sensor and keeping transmittivity to THz waves, which means no conductive components can be applied. The physics involved in the dielectrostriction of

our composite and the different effects on the ToA are explained further and developed mathematically in section 3, which proposes a theoretical model of the sensing process.

CHAPTER 2. LITERATURE REVIEW

The literature review has been divided into two subsections, the first one contains an explanation of the main state of the art strain mapping methods used today, explaining pros and cons of each, highlighting important recent research, and comparing them with our sensing method. Then, a literature study is also performed of different methods of sensing strain with THz spectroscopy, and how they compare to the proposed in this work.

2.1 State of the Art Techniques of Strain Mapping

2.1.1 Strain Gauges

Strain gauges consist in attachments to the surface of components that can provide information of the local strain state of the surface to which they are attached. They basically operate by deforming in the same quantity as the substrate, which will produce changes in its physical properties that can be quantified through different analytical methods. The sensor that has been developed for this thesis can be considered of this type since it requires an attachment to the specimen to be measured.

Strain Acoustic Wave Sensors

Surface Acoustic Wave sensors have potential in strain sensing applications due to the high reliability and precision they possess, together with the ability to be used in passive sensing if designed for this purpose. Surface Acoustic Wave sensors (SAW) can sense changes in several phenomena of the substrate to which they are attached by quantifying differences in mechanical acoustic waves that go through this substrate. Their functioning consists in the transformation of a received electromagnetic signal into an acoustic wave that will go through the surface of a substrate

by means of an interdigital transducer (IDT). Depending of the way this electromagnetic signal is produced and transmitted to the IDT, a passive sensing method can be obtained, for example when using an antenna [13], [14]. During the emission in the IDT and transmission of the acoustic wave along the substrate, it will suffer changes on phase, frequency, phase, or time-delay, which can be correlated to different parameters of the substrate through previous calibration. The presence of cracks and heterogeneities will further affect the transmission of acoustic waves. Afterwards, the wave is received by the interdigital transducer and transformed back to an electromagnetic signal which will be used to analyze the property studied, which could be pressure, strain, force, mass, etc.

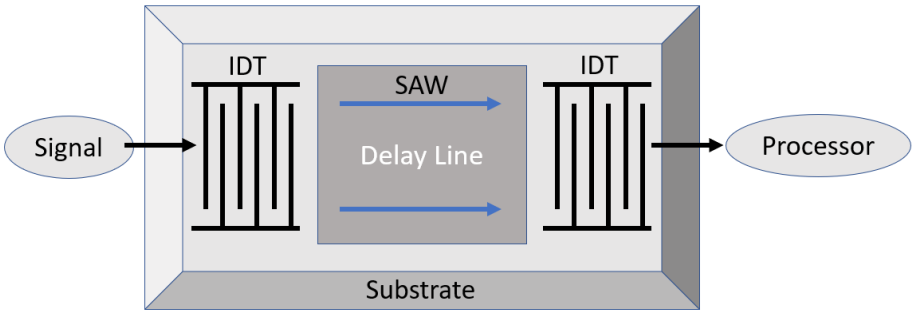

Figure 5: Schematic of Surface Wave Acoustic sensor showing the emission, propagation and reception of a Surface Acoustic Wave.

These substrates will consist of piezoelectric materials, which produce an electromagnetic potential or voltage when they are under stress, and vice versa, they will produce a force when a voltage is applied to them. Therefore, the interdigital transducer will use this effect to convert the given electromagnetic signal into acoustic mechanical waves through a periodically distributed signal. In order to measure the strain of structural components, the SAW sensors are attached to the structural component to be monitored, and the strain in the component will produce changes

in the acoustic waves through variations in the IDT geometries and the area of propagation. Another important advantage of this type of sensors is that they can also include additional filtering to indirectly sense some different phenomena at the same time. All the mentioned advantages make SAW sensors very appropriate for structural health monitoring in industrial applications; however, even though the electronics used can be very compact, they require a propagation surface for the acoustic waves, which make them lose spatial resolution with respect to other strain sensing techniques, that together being able to sense only unidirectional strain. Nonetheless, such sensors are increasingly being used for health monitoring applications in several industries due to their sensitivity and passive sensing potentials; for example, [15] reports the design of a passive SAW capable of detecting 0.01mm cracks for aeronautical structures by using Orthogonal Frequency Coded Reflectors. When comparing it to our THz sensor, it may come on top due to the SAW not having a high resolution since it needs some propagation space for its delay line and it only being able to measure unidirectionally; however, these sensors are highly reliable and are widely used for many applications.

Optical Fiber Strain Sensors

Optical fiber methods for strain sensing benefit for its immunity to electromagnetic interference and the ability to operate at a wide range of temperature compared to other type of strain gauges. Although there are several methods to pursue strain sensing through an Optical-Fiber, they all mainly focus on studying changes in the properties of a light signal that goes through the fiber as it is being stretched or compressed. The main sensing approaches that could have strong potential in studies at the mesoscale are scattering methods, which measures light scattering strain-sensitive behavior along an unmodified optical fiber, and Fiber Brag grating, which quantifies spectral shifts in the light of the fiber by the application of wavelength selective mirrors

throughout the fiber. The former provides fully distributed measurements without many modifications, since changes in scattering are produced by the local strain-sensitive optical properties of the fiber, but they suffer in precision with respect to the grating methods, which are able to provide much more reliable measurements by applying accurate modifications on the fiber, which increases a lot the sensitivity to strain of the measured parameters. However, for the latter it is harder to provide high fidelity strain maps, whose spatial resolution will depend of the type of grating that can be applied, but there are several commercially available that use this method and are able to provide precise measurements with a few millimeters of spatial resolution.

Fiber Brag Grating

This technique applies a distribution of Bragg reflectors in a segment of the optical fiber with the objective of reflecting particular wavelengths of the light that go through it, while transmitting the rest of them; this allows to measure differences in the reflected light at a particular wavelength, therefore being able to locate the measured change along the fiber. Although this method will usually achieve lower spatial resolution than its scattering counterparts since the gratings requires some distance for appropriate distribution, they are able to produce very long and thin sensors with high potential in industry, while also showing better performance when measuring dynamic measurements due to the higher time-resolution of light. Ref. [16] reports the development of a high spatial resolution FBG sensor that allows to measure along a 10m distance with a 1.5mm spatial resolution. These sensors usually have higher sensitivity than SAW but also show a lower spatial resolution than THz waves, they are also not wireless, so THz sensors could be more useful in many applications where optical fiber can’t be attached to the structural component requiring measurement.

Rayleigh Scattering Distributed Strain Sensors

The scattering method that can produce the smallest spatial resolution uses Rayleigh scattering. This is a type of linear scattering that happens due to microscopic imperfections in the fiber, which produces variations in the refractive index and stronger signals compared to non-linear scattering that allows them it to achieve a better spatial resolution.

In order to produce a spatially distributed measurement of the back-scattered light, interferometric techniques are used through Optical Frequency Domain Reflectometer coupled with a Mach Zehnder interferometer, which are based on a superimposition of the light that is reflected from the strained fiber over light that is obtained directly from the sent-out source. This way, the scattered light interferes with the reference light from the same source and varying the frequency with the source will produce periodic signals at the detector, whose frequency will depend on the position of the obtained scattered light. Then, since the detector is receiving the backscattering signal from several positions at once, the frequency components have to be split through a Fourier transform, which will yield the position of the fiber for which each scattering amplitude is being measured, and the intensity of each scattering will be given by the amplitude of each frequency, which will be a function of the strain at that position.

This method allows to obtain distributed measurement of small strains of about 1 microstrain with mm spatial resolution throughout long distances of a few dozens of meters. However, in this methods the limits are not set by the physical characteristics of the different components involved, since the signals are produced by local properties of the fiber and measured using lasers with very high spatial resolution; the limits in resolutions are set by the intricate analytical procedures of the complicated signals that are generated, therefore if the specific application requires less measured surface and time-resolution, one could produce measurements with finer spatial resolution, which implies that there is a lot of research potential in mathematical

spectral analysis to improve the capabilities of this method. Research is active for this method and some authors are already showing improvements in spatial resolution. For example, ref. [17] shows the development of a reflectometry method that produces a breakpoint detection with 0.1mm. Although this method will have higher spatial resolutions than THz sensing, THz waves offer the advantage that they can go through opaque materials while optical beams cannot.

Radio-wave strain sensors

The techniques disused till now lack the ability to perform passive sensing from a long distance. Although, some of the techniques perform non-contact sensing and can provide passive sensing in a close range, they cannot provide long distance remote sensing abilities as radio-wave sensors. Passive radio-wave sensors present the opportunity to perform through non-metallic barriers due to penetration by radio frequencies. The schematic of radio frequency-based sensing system is shown in **Figure 6**.

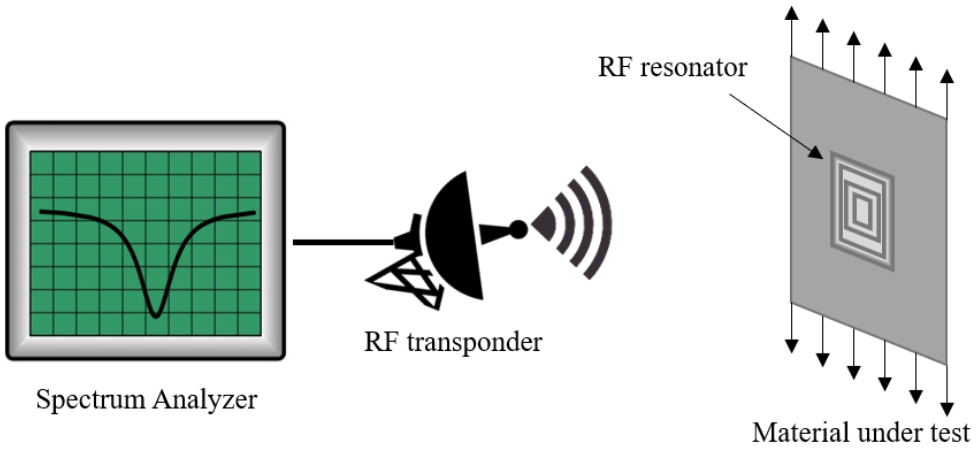

Figure 6: Radio frequency sensing schematic.

The sensor is made in a form of radio frequency resonator whose resonance frequency changes under the application of stress, either by change in length of the resonator or by change in dielectric

properties. The change in resonance frequency is detected via sweeping the frequency range using a radio frequency transponder and a spectrum analyzer. The use of radio-waves using surface mounted radio frequency transducers for strain sensing has been demonstrated by few researchers [18], [19]. The other radio-wave sensors uses change in dielectric properties of coatings made from materials such as strontium titanate and barium titanate to observe change in stress state of a material [10], which has a similar basis to our technique. However, it must be noted this kind of radio-wave sensors have not been used extensively. They also do not show very high spatial resolution, since the attachment of antennas requires some space, and the sensitivity obtained in their current state is limited. Furthermore, radio-waves do not transmit as well as THz waves, which may prevent them from being used in some applications.

2.1.2 Optical Whole-Field Techniques

These techniques consist of obtaining accurately the whole distribution of strain along a structural component using continuous imaging methods. They are based in sensing differences in the images taken as the specimen is being stressed and can quantify its strain along all the graphed part of the specimen through different analytical methods. Optical Whole-Field techniques are getting a lot of importance in materials characterization since those are passive sensing methods that allow to quickly measure accurate strain fields. These can also be used in almost any material at fast strain rates, and at environments where other sensing methods may present problems. Furthermore, mostly they do not require attachments to the material and produce faster measurements than THz TDS spectroscopy for imaging since as of now there is no technology to measure several points at the same time and the mapping needs to be carried out pixel by pixel, which can be a lengthy process, however for optical techniques opaque materials like casings can’t be in the optical path while that is allowed for THz TDS mappings.

Holography Strain Sensing

Holography is the process of recording and reconstructing the complete optical wave front reflected from an object, which uses principles of interferometry to measure phase information in addition to intensity information, which is the only parameter obtained in photography. The application of holography to interferometry makes possible to study three dimensional diffusely reflecting objects with non-planar surfaces, where classic interferometry only works on secularly reflecting flat surfaces. Under proper analysis, the obtained fringes can yield information about the components of the displacement vector all along the analyzed surface, which can then be used to imply stress components if it is carried out in conjunction with photoelasticity.

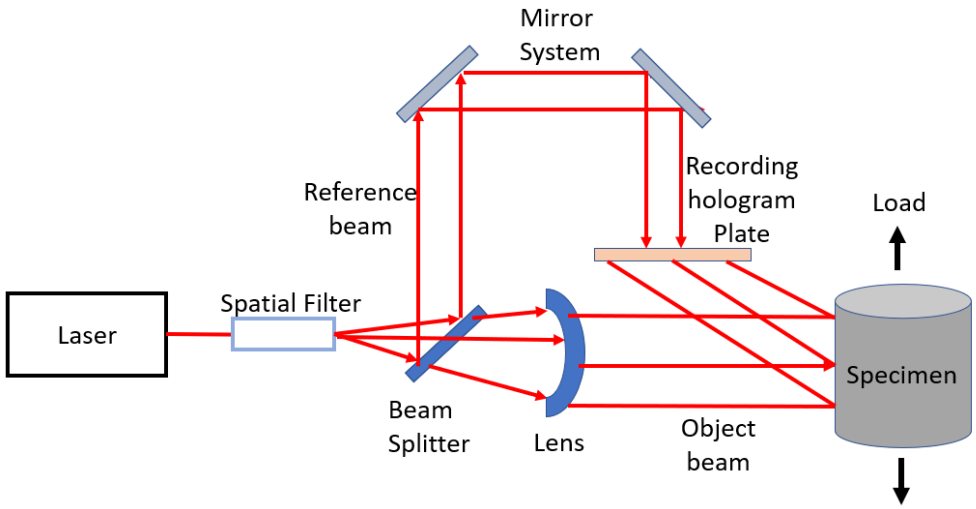

Figure 7: Optical Set Up of holography for strain measurements.

In order to obtain the phase information, the procedure consists of superposing two laser beams, one being a reference obtained by splitting part of the laser beam before it reaches the body, and the other coming from the reflection of the body to be analyzed. This will produce a holograph of the three-dimensional body, which can be recorded and compared to another holograph obtained

the same way once the component is deformed. The comparison between the two holographs will yield the fringes that were desired to obtain the displacement information. To study strain fields with this technique, one has to find a correlation between the fringe behavior and displacement, which requires complicated analytical methods and high environmental stability, since the vibration behavior of the specimen could highly affect the readings, as well as external light sources and instabilities in the optics. However, this method yields the highest sensitivity among all the optical whole-field techniques that will be described in this paper, which explains the importance these methods have in the study of micro electro-mechanical systems and shows it has strong aptitudes to be used in mesoscale studies. Holography can also be performed using electron waves in a method called dark field electron holography, which allows to reproduce the same procedure as explained before but using electron microscopes, performing a displacement analysis of a small region with nm resolution in semiconductor devices. A lot of advancements are happening in this area since there have been important developments in higher quality electron microscopes. Ref. [20] explains this method thoroughly in case the reader in interested in the specifications. Ref. [21] reports measurements applying a dual lens configuration, which produces strain maps below nm resolution with variable magnification that permits adjusting the field of view. Furthermore, [22] develops a technique that also allows to measure the derivative of the phase in the holograph, allowing for higher accuracy in the measured strain distributions.

Moire Method

Moire method refers to sensing through the application of a fabric on the substrate and a reference fabric that superposes two identical gratings, such that when the substrate grating deforms, it produces the apparition of light and dark patterns, also called fringes. This is called the Moire

effect, which is graphed in **Figure 8**. These fringes can then be used to extract information regarding the displacement field of the surface of the substrate to which the fabric is attached.

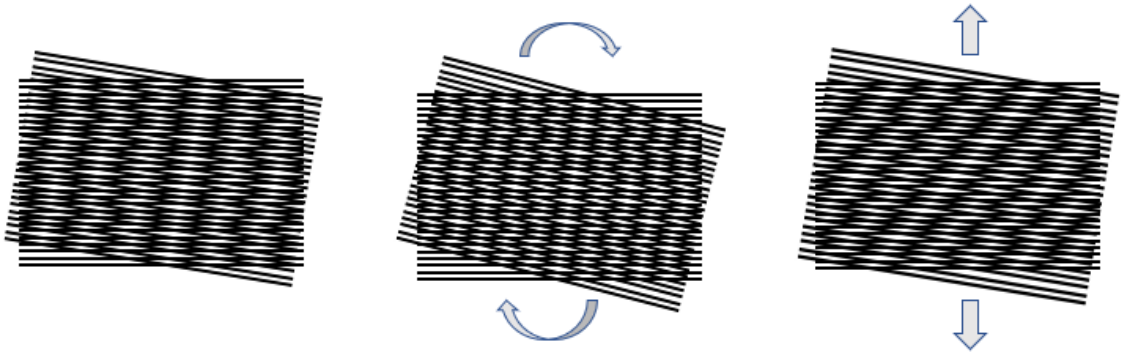

Figure 8: Principle of More method, showing how the superposition of two gratings produces fringes and how the specific deformations in one of the gratings will affect the fringes observed.

Summarizing this measuring technique of this method is complicated because there are a lot of variations depending on the required application, but they all coincide in that they require an implementation of superposed geometrical patterns on the substrate surface that will produce sensitive enough fringes. Ref. [23] performed a thorough analysis of the different Moire techniques available that are used for deformation analysis, which is recommended to the reader if more information is wanted. In order to simplify, those could be divided into two subgroups: Geometric Moire and interferometry Moire. Geometric Moire is based completely in changes if geometry, and interferometry also takes into account diffraction effects, which allows it to achieve higher sensitivities but involves a more complicated procedure involving smaller geometries and an optical interferometry set up. In Interferometry Moire; however, the reference grating is not a physical grating that is being superposed with the substrate grating in the field of view, it is instead a virtual image obtained by splitting part of the laser to a mirror before it reaches the specimen. Geometric Moire is usually the method employed for gratings with 40 lines/mm or above, which

allows for a maximum resolution of 25 micro-strain, interferometry Moire is required for analysis of finer gratings. However, it must be noted that interferometry Moire can only be applicable to planar surfaces and measures only in-plane displacements, where mechanical can measure out of plane displacements and works on curved surfaces.

Although mechanical Moire method may struggle to yield very high resolution, it has proven to be quite useful in industrial applications of larger specimens due to its simple implementation and low-cost. On the other hand, Moire methods based on interferometry have yielded very high spatial resolutions with fast measurements, so their industrial applications focus on smaller scales like analysis of electronic packaging, and they can be quite beneficial for researching material properties at the mesoscale in lab environments. Several methods have been reported to yield fast sensing of full strain-fields with impressive spatial resolution, especially if microscope systems are implemented in the interferometry, which yield pixel sizes in the nanometer range. The different current applications for Moire interferometry are explained in ref. [24]. Regarding late improvements, ref. [25] proposes a method of automatically measuring full strain fields with a 164nm spatial resolution using a two-level imaging system

Laser Speckle Methods

The surface of most materials is rough at light wavelength scales even though they seem virtually specular, this means that when they are reached by a coherent light source like a laser, they will reflect randomly distributed speckles which will be characteristic of a given surface, like a fingerprint. This fingerprint will be constant in space and time if the light source and surface are unaltered, and therefore will be displaced in the case of surface strain. Laser speckle methods consist of illuminating the surface of an object through a coherent laser and then studying the displacement of speckles formed in the reflection using interferometry methods. This method

could be considered a branch of holographic interferometry since they use the same optical set-up, but it offers the important advantage that speckles can be easily graphed using modern digital cameras, where holography requires a high-resolution recording medium.

They can be classified in objective and subjective speckle methods. In objective speckle methods, the light reflections from several points add up constructively and destructively to yield an speckle in the measuring screen. In subjective methods, a lens is used in order for the scattered waves from a single point to be focused on a corresponding point in the image. Subjective methods yield speckles that are easier to study and therefore are preferred for practical applications.

Besides of using a simpler recording sensor, speckle methods also offer the advantage that the double exposure technique is applied using digital methods and therefore real-time sensing of the fringes can be performed, measuring displacements at relatively fast strain rate, and the only requirement for surface preparation is the application of a paint or spray that can yield speckle information. This method is mostly used to study out of plane displacement information, but with specific arrangements and data analysis techniques it is possible to measure in-plane displacement.

The achievable spatial resolution is of a few microns, which will depend not only of the optical capabilities, but also on the data analysis method used, ref. [26] provides a good explanation of how signal processing of Laser Speckles for strain measuring works. Ref. [27] explains how a laser speckle method with resolution of 50nm was achieved using a laser speckle correlator with high optical magnification.

White Light Speckle Digital Image Correlation

In white light speckle methods, displacement analysis is also performed by studying speckle movement with digital cameras. But in contrast with laser speckle methods, here the speckles are applied artificially to the sample surface and can be seen with white light, so the reflection of

coherent light is not needed. This allows to obtain strain measurements without using intricate optical setups, but involves a much deeper data analysis using advanced statistical techniques in order to interpret correctly the experimental data, which is needed to yield accurate results with high spatial resolution, which is why it also receives the name of Digital Image Correlation (DIC). Ref. [28] and [29] explain how data analysis for DIC correlation work, while comparing several methods that are currently used.

However, this method uses surface preparation techniques that are usually easy to apply and produce no effects on the material, which makes possible to produce non-contact analysis for almost any material in a very wide range of applications. It can also be used to measure in a wide range of length scales depending of the recording sensor chosen, which could also include different types of microscopes for studies at the nano-scale. Furthermore, it can be used to find all components of displacement, and together with its versatility, it is becoming very attractive to characterize material properties through strain mapping. Nonetheless, it still struggles with achieving high accuracy and reliability, so there is room for improvement, but its high potential explains why it is attracting so much research emphasis in material science and statistical data analysis. Recently, several publications have reported using this technique in combination with other method to produce newer capabilities, ref. [30] uses volumetric speckle photography with X-ray microtomography to increase accuracy.

Photoelasticimetry

Photoelasticimetry consists in studying stress distributions through the stress-sensitive optical properties of certain materials. These materials, called birefringent materials, are characterized by the change from an optically isotropic state to a doubly refractive behavior when they are stressed. These changes can be studied through the emission and reception of a linearly

polarized electromagnetic wave that goes through the photoelastic materials with a polariscope; as it goes through this artificially anisotropy induced by stress, the polarization state of the wave will be affected by an interference in phase directly proportional to the principal stresses at a given point, which allows to measure the magnitude and orientation of principal stresses and produce high fidelity stress maps in real time.

Measurements can either be done in transmission or reflection configurations, the former is usually used for model studies since it yields more accurate measurements but can only be used on specific birefringent materials; reflection, on the other side, allows to apply this measuring technique to opaque materials through the implementation of a birefringent coating, the electromagnetic wave will pass through this coating before bouncing on the substrate and going back to the analyzer. However, besides this last procedure being more intricate, it only allows to quantify strain and not stress in the substrates, acting more like a strain gauge where the stress on the photoelastic coating is transmitted from the substrate through adhesion. Ref. [31] proposes a method to measure stress through the birefringence sensing of sol-gel coatings. Recently, photoelasticty has also been exploited to measure optically opaque materials through THz spectroscopy, since electromagnetic waves in this frequency range are able to penetrate most dielectric materials [32], this is explained later in the strain sensing methods through THz TDS section 2.2.1 .

2.1.3 X-ray diffraction

X-ray diffraction is a mature non-destructive technique that has been widely used in industry for the detection of residual near-surface stresses in polycrystalline solids. It measures strain in the crystal lattice through changes in the Bragg diffraction of the strained region. Bragg diffraction happens when intense electromagnetic radiation, with wavelengths in the scale of

atomic spacings, scatters in a specular manner from the lattice planes, and suffers a constructive interference. This interference will be proportional to the incidence angle and the distance between the lattice planes, which allows to calculate the distance of the crystallographic planes and can be correlated with strain. This can be understood through Brag's law given by **Eq. (2)**, where θ is the glancing angle, k is a positive integer, d is inter-planar spacing and λ is the wavelength.

$$2d \cdot \sin(\theta) = k\lambda \qquad \textbf{(2)}$$

However, Poisson's ratio effect also produces a change in Θ besides a difference in planar distance, so in order to produce the measurements, one has to measure the sample at two different orientations for the same loading state, so the value of θ can be obtained. This method has a lot of applications since it does not require any surface preparation and can measure strain accurately with high resolution. Another characteristic to be noted is that crystal plane spacing only yields information about elastic strain, which allows it to be correlated with stress through elastic constitutive laws, but it is not possible to measure beyond yield point since it produces dislocation displacements and the crystal lattice is disrupted. Furthermore, another downside is that it uses ionizing radiation, which requires extra cares to be taken in designing the measuring method to prevent radiation exposure. This method can also be used in high temperature applications, [33] uses this method to map internal strains of thermal barriers during thermal fatigue loading. This method can also be applied in microscopes to produce high-resolution strain scanning, ref. [34] provides an explanation of how this method is produced together with high-resolution mapping in three dimensions.

X-ray diffraction is more mature than THz, has higher resolution and can penetrate opaque materials, but it has the disadvantage that it uses ionizing radiation and therefore requires to take steps to protect personal in its use. It also measures axial strain of an individual crystal so it is intricate to determine homogeneous strain.

2.1.4 Raman Spectroscopy

Raman spectroscopy is a molecular spectroscopy technique that analyses the inelastic scattering of phonons or molecular vibrations. While Rayleigh scattering refers to elastic scattering, which is most of the scattered light and has the same wavelength as the source, Raman scattering is made of inelastic scattering, a much smaller amount of the scattered light that is characterized by a different wavelength than the source. Through the value of these wavelengths, important information can be extracted from the matter where the light is scattered.

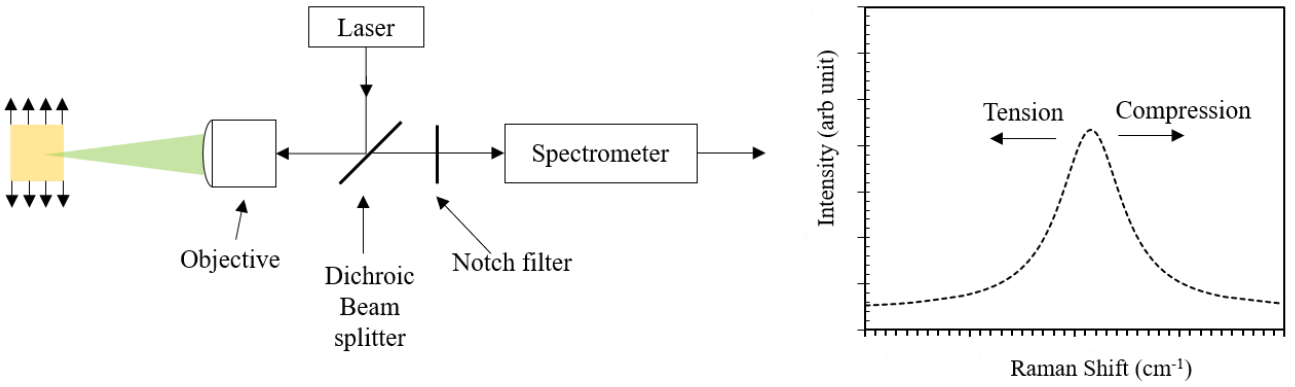

Figure 9: Schematic of Raman spectroscopy together with the obtained results, and how compression or tension of the molecular structure will produce shifts in the Raman peak.

Initially, Raman spectroscopy was mainly used for chemical studies or solid-state physics like the analysis of a specimen phase composition. But eventually, it was discovered that a lot

more information can be found in the yielded spectra, one of them being the stress-state of the scattering surface along with temperature [35].

Stress has an effect on Raman-active phonons and molecular vibrations, which produces a shift in the measured wavelengths at which inelastic scattering happens. This relation can be calibrated and then used to measure near-surface stress easily in a variety of applications. **Figure 6** shows the schematic of a Raman Spectroscopy Set up and stress effect on the results.

The amount of Raman peaks available for study depends on the material that is being analyzed, but for certain materials it is possible to produce 3D stress field analysis. Raman spectroscopy is not possible on metals since their molecules do not show a change in polarizability during molecular vibration, but recent research has shown the ability to measure stress in metallic surfaces by using a silicon coating on metallic substrates that will deform the same way as the attached metallic component [36] .

The achievable spatial resolution of Raman spectroscopy depends on the spot size of laser beam on the samples, but it is usually in the sub-micrometer range. The main advantage of Raman for stress analysis is that it offers a sub-micrometer resolution technique that is relatively cheap and simple to implement and is widely used in research for material studies. Raman spectroscopy has also been used at nanosecond time resolution using time-gated Raman spectroscopy to analyze stress included due to shock propagation [37]. Although Raman spectroscopy has many advantages such as high resolution and the ability to measure Von Mises Stress, it has the disadvantage that as for other optical methods they are blocked opaque media.

2.1.5 How THz TDS stands as a strain sensing method

As can be seen from this literature survey, not many methods allow to perform strain measurements in regions that can’t be reached through cables or by optical beams. The only

methods that can accomplish this purpose are strain gauges that have been applied an antenna and are able to communicate strain passively through radio waves, or by x-ray diffraction measurements. However, as previously explained, antennas require space which limit their spatial resolution and are usually attached to components that measure axial components, also radio waves do not transmit well through certain media and have bigger wavelengths than THz. Regarding X-rays, they produce harmful ionizing radiation and are only able to measure the local strain of a lattice, which makes hard to obtain strain mappings of bigger regions.

2.2 Alternative Methods of strain sensing through THz TDS

This subsection talks about different methods that have been developed to capture strain through THz TDS methods and how they differentiate from the one being developed by this thesis. It must be noted that all these methods are of fairly recent discovery and none of them are well established nor used widely in industry.

2.2.1 Plane Stress Measurement through birefringence sensing with THz TDS

Measurement of plane stress through the sensing of birefringence has been accomplished and published in the literature. These works make use of the stress-optical law to determine the plane stress of a material by correlating a phase-delay of the received THz wave and the birefringence it is experiencing due to stress.

Ref. [32] accomplished this on PTFE, an optically opaque material, by applying two polarizers to a conventional THz TDS system. This makes possible to receive only waves with a predeterminate polarization. The stress-optical law proposes that when an optically isotropic material is strained, a state of anisotropy is induced where the optical axes of birefringence that is produced will align with the principal stresses that the material is experiencing. This way,

depending on the polarization angle of the wave, it will experience a higher or smaller index of refraction n, being the highest and lowest if the polarization is aligned with the principal stresses. This change in index of refraction will produce a phase-delay in the THz wave that can be quantified through the time domain spectroscopy, and by changing the polarization state one can obtain the value of the principal stresses and its direction and determine the plane stress of a material.

When comparing to our methods, this technique is quite useful since it can determine the whole plane stress state, while we can only quantify volumetric strain. However, this method requires to apply two polarizers and rotate them to produce the measurements, which complicates reasonably the procedure in case it had to be applied to industrial applications. Measuring volumetric strain with STO composites would not require doing this, meaning the procedure could be easily automatized, but only allowing for a qualitative analysis since not all the strain matrix can be measured. Furthermore, measuring strain through polarization does not yield a linear response and its sensitivity is not very high, with some error appearing in the measurements, meaning it is not going to have much use besides research applications. One utilization of this technique is to measure internal strain of black rubbers, which is first measured and reported by [38] to show important birefringence through THz TDS, and then it is explained by [39] that it is due to the reorientation of inclusions inside it; which could have important applications in NDT of the material. However, there is no literature in using this principle for sensor development.

2.2.2 Strain Measurement through THz TDS of passive Metamaterial

Other reported method to measure strain through THz TDs is by the utilization of a metamaterial strain gauge. Metamaterials can be defined as synthetic composites with a determined structure that allows the manipulation of electromagnetic waves in unique ways.

Superlenses [40], perfect absorbers [41] and stealth cloaks [42] for military use are common application of metamaterials.

For the purpose of strain measurement through electromagnetic waves, there is a fair amount of literature that uses microwave metamaterials, the most common being the use of split spring resonators that relate resonance frequencies to strain [43]. Lately, this work has been expanded to THz waves due to the advantages that we explained through this thesis, although the work is similar, just requiring modifications to the geometries and materials in the metamaterials to be used [44].

These sensors are based in using sub-wavelength conductive architectures to produce a resonance at a specific frequency in the THz waves that probe it. The frequency at which the waves resonate will depend on the geometry of this sub-wavelength structure, that will be changed by strain, shifting the resonance frequency, which can be sensed and therefore correlated to strain[44].

Sensing strain with this technique yields good sensitivity, although the change of strain with resonant frequency is non-linear, which complicates calibration. Furthermore, although it has been demonstrated that strain from different directions will produce a different shift, it is not possible to know exactly how several strains will affect the shift so exact quantities cannot be determined. Regarding published applications used for this sensing method, ref. [45] shows how this sensors can be useful for studying opaque composite materials and reports a strain imaging.

CHAPTER 3. 2D VOLUMETRIC STRAIN IMAGING THROUGH THZ TIME-DOMAIN SPECTROSCOPY OF STRONTIUM TITANATE FLEXIBLE COMPOSITE ACTING AS REMOTE PASSIVE SENSOR

Luis M. Reig Buades[1], Abhijeet Dhiman[1], Vikas Tomar[1,*]

[1] School of Aeronautics and Astronautics, Purdue University, West Lafayette, Indiana 47907
*Corresponding author, Phone: (765)-494-3006 Fax: (765) 494-0307 Email: tomar@purdue.edu

Manuscript under preparation

Abstract

Terahertz Time-Domain Spectroscopy (THz TDS) is a high-resolution and low-absorbance novel spectroscopic technique with important potential for strain imaging applications through opaque media, which could prove useful for applications in the fields of material characterization and structural health monitoring. The following work analyzes how attaching a composite of Strontium Titanate (STO) particles dispersed in an elastomer matrix to a structural component, a material that changes its dielectric constant when loaded, and sensing the change in dielectric properties of the coating at different loadings, a new non-destructive and remote sensing method of strain field mapping can be achieved. This method has made possible to correlate strain to changes in the time of arrival (TOA) of a THz EMP that goes through the sensor, and then use this correlation to measure the localized strain field around different geometries through previous material-specific calibration, which are reported in this document together with a mathematical modeling of the physics involved in the sensing process.

3.1 Introduction

The following study analyses how the application of a flexible coating with high dielectric constant and dielectrostriction, meaning that its dielectric constant varies with strain, to a structural component, could produce a passive sensor for the measurement of strain fields. This coating is composed of Strontium Titanate particles (STO) in a PDMS matrix. By dispersing STO, a high dielectric material that is already dielectrostrictive by itself, in PDMS, an elastomer with low

dielectric constant, a flexible composite is obtained with high dielectric permittivity and dielectrostriction coefficient. When probed through an Electromagnetic Pulse (EMP) in the THz frequency, this effect will produce changes in the velocity of the THz pulse that goes through it. These changes can be measured and correlated to strain through THz TDS due to its special dielectric behavior. By taking advantage of the high resolution of electromagnetic waves in the THz spectra and their capacity to go through a wide range of materials, this approach makes possible to measure the strain state of components even when there are opaque materials in the THz wave path, as long as they are transparent to THz waves, which includes most polymers and ceramics. This analysis yields a novel contactless structural health monitoring technique that also allows for sensing of components inaccessible through other non-destructive methods if they are obstructed by opaque media.

This approach could prove better for certain sensing applications than the optical methods currently used to measure strain fields because THz waves are able to penetrate through many opaque materials, which would allow to study components unreachable by optical methods. Regarding using it as a wireless sensor for structural health monitoring, work in the development of THz strain gauges for structural health monitoring has already been realized by applying frequency selective metamaterials that change their resonant frequency when deformed [46]. This method measures axial strain, our approach instead measures volumetric strain through a change in wave speed as the coating is stressed and the refraction index of the media changes, which involves simpler and less expensive manufacturing.

The following work analyses mathematically the different physical phenomena that will affect the THz wave when the sensor is strained, producing an analytical model to calculate an increase in the measured ToA (ΔToA) for a given 2D volumetric strain. The effects of strain in the

sensor that affect the THz pulse velocity are a change in thickness, a dielectrostriction effect by the rearrangement of the high dielectric STO particles inside it, and also another dielectrostriction effect by the stress on STO itself. These are all analyzed to yield a linear relation between ΔToA and strain. Afterwards, experimental measurements of ΔToA through THz TDS are obtained for different strains, which also show a linear relation with results like those yielded by the analytical model. Finally, the yielded linear correlation is used as calibration to produce strain mappings of different geometries that produce localized strain, showing how this method could be used for strain imaging.

3.2 Theoretical Modeling

The following section contains a theoretical modeling of the physics involved in the strain sensing method developed in this work. Although the theoretical model yielded is not used in the measurements, since those require a pre-calibration due to usual differences between the practical and theoretical measurements, it can be useful to quantify how different parameters of the sensor structure will affect its sensitivity. This can help to understand how changing the different characteristics of the model such as thickness, particle density or matrix material can affect the sensitivity of the sensor, yielding how changes in the sensor parameters will produce higher or smaller changes in Time of Arrival (ToA) with strain. Regarding the measurement technique, it consists of applying **Eq. (3)**, where we are calculating the volumetric strain at a given point (e_{vol}), which has this notation since ε is used for dielectric constant, through multiplying the change in time of arrival (ΔToA) by a constant (C). This constant is obtained through previous calibration of a tensile test that shows a linear dependence between ΔToA and e_{vol}. For a tensile test, $e_{applied}$ can be known since it is the applied extension with the loading stage divided by the gauge length.

Then, e_{xx} can be calculated by Poisson's ratio. If Poisson's ratio is unknown, a suggestion for calibration would be to use digital image correlation to measure the strains instead of the loading stage data.

$$e_{vol} = e_{xx} + e_{yy} = e_{applied} * (1 - v) = C \cdot \Delta ToA \quad \textbf{(3)}$$

This would be enough knowledge to be able to produce a strain mapping with this method. The theoretical analysis will explain how this relation arises, and why it only allows to measure 2D volumetric strain instead of other strains in the plane strain matrix. Furthermore, the mathematical model obtained will allow to produce different studies of how changing determinate characteristics in the sensor would increase or decrease its sensitivity, and how this can guide its design process.

3.2.1 Velocity of electromagnetic radiation in dielectric media

Since we are measuring delays in ToA of arrival in a THz wave going through polarizable media, it is essential to understand how the velocity of the wave will change along the different media that it travels from its emission to its arrival at the receptor. If all the velocities and distances that the wave travels in each media were known, it would be possible to analytically calculate the ToA by means of **Eq. (4)**, which can be understood through **Figure 10**.

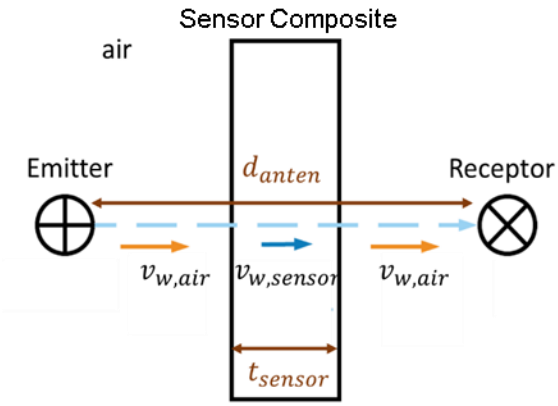

Figure 10: Visualization of the variables that kinematically are going to affect the time of arrival of the THz wave to the receptor in a transmission configuration. If all these variables were known, the time of arrival could be analytically calculated through basic kinematics.

$$ToA = \frac{d_{anten} - t_{sensor}}{v_{w,air}} + \frac{t_{sensor}}{v_{w,sensor}} \quad \textbf{(4)}$$

Experimentally, there will be some transitory processes such that the wave velocity will not change instantly as the wave changes its media of propagation; however, for most theoretical models the change happens so fast that this assumption ca be carried out, so we will have two different wave velocities in our model, $v_{w,air}$ and $v_{w,sensor}$, which will correspond to the wave velocity in the air and in the sensor respectively.

According to the electromagnetic wave equation, the phase velocity of an electromagnetic wave (v_w) in a ‘‘simple’’ material is given by **Eq. (5)**. This equation implies that the velocity of the wave traveling this media is dictated by an inversely proportional relation between the speed of light in vacuum (c) and the dielectric (ε_r) and magnetic (μ_r) permittivity of the material it is traversing.

$$v_w = \frac{c}{n} = \frac{c}{\sqrt{\varepsilon_r \, \mu_r}} \quad \textbf{(5)}$$

It is important to understand that this equation applies only to ‘‘simple’’ materials, what that means and if we can consider our composite as such. According to its definition, a simple material implies a media with no charge, non-conducting and where ε_r and μ_r are constants; but that is also homogeneous and isotropic, the former meaning that the direction of travel in the material does not matter and therefore has translational symmetry, and the latter meaning that there is full rotational symmetry.

Regarding our sensor, ε_r and μ_r can be considered constants for the purpose of this model as it is explained in the following subsection (3.2.2), it also has no charge density and it’s non-conductive since its components are dielectric. However, our material will lose its homogeneous and isotropic properties when it deforms due to the particles displacing with strain, meaning the direction of propagation and polarization of the wave will influence its velocity through the media. Luckily, for our experiments the electromagnetic wave always propagates in the same direction, from the emitter to the receptor, and the waves we are using are unpolarized, so the assumptions can still be carried out, this is justified with more detail in section 3.2.4.

3.2.2 Electromagnetics properties of sensor composite

Once it is clear the ToA is going to be dependent on the electromagnetic permittivity of the different media it travels, the next step is to understand what are the different permittivities that the THz wave is going to experience during the measurements.

Regarding air, it has a very low dielectric permittivity that will vary with temperature, humidity, and pressure; regardless, it is usually considered equal to 1 in the literature for procedures like ours. With respect to its magnetic permeability, air is non-magnetic so it can also be considered unity. With these properties, **Eq. (5)** yields that air will have a unity index of refraction (n) and the velocity of the THz wave traversing it will be equal to the speed of light in vacuum ($v_{w,air} = c$) for this model.

When looking at the electromagnetic properties of our composite, both of its constituents must be analyzed to understand its overall dielectric properties. Firstly, with regards to the magnetic permeability, both the polymer used (PDMS) and STO are diamagnetic materials, meaning they experience that is a property of all materials ($\mu_r < 1$), but this repulsion is usually too low to be considered for non-ferromagnetic materials, which can be seen in **Eq. (6)**, where their magnetic susceptibilities χ_v are so low that the permeability of the composite can be considered unity.

$$\mu_r = \chi_v + 1 \quad \rightarrow \begin{cases} \chi_v sto = -6.72 * 10^{-6} \\ \chi_v pdms = -1.07 * 10^{-6} \end{cases} \qquad \textbf{(6)}$$

With reward to the polymer matrix, polymers are usually pure dielectric materials, meaning they respond with a linear polarization to an electric field, so they will have a constant ε_r and it should not be affected by deformation.

As for the STO, in its non-doped state at room temperature, it is a paraelectric materials. Polarization of paraelectric materials can be understood looking at **Figure 11**. In contrast to dielectric materials, its polarization is non-linear, which is usually a property of materials with

very high dielectric permittivity; nonetheless, it can be seen that for a given magnitude of electric field it will always reach the same the same polarization so its ε_r can be also treated as a constant, since it does not show polarization memory. This would not be the case of a ferroelectric material, which usually show the highest relative permittivities, but since they show dielectric memory they are not useful for this sensing method due to the polarization experienced for subsequent electromagnetic fields not being the same. This is the reason why STO is optimal for this technique and it's such a used material for microwave applications, since it has a very high dielectric permittivity but, unlike the rest of Perovskites, it has paraelectric properties and it does not exhibit polarization memory. However, it must also be mentioned that for some ferroelectric materials, if the electric field is of low magnitude, not enough dielectric memory is experienced in the material. This could allow for ferroelectric materials to be used in this method, since THz spectroscopy uses low magnitude fields, so there may be other material combinations that could exist to produce a high dielectric constant.

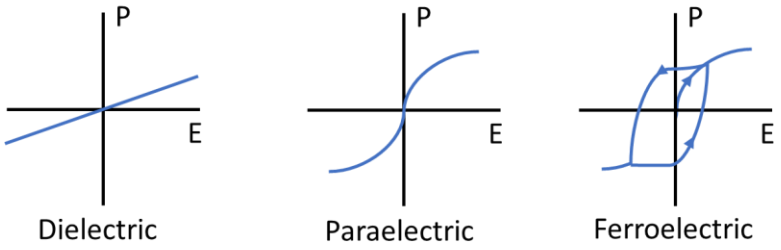

Figure 11: Material classification depending of their polarization response to an electric field.

Then, since the magnetic permeability of both constituents can be considered unity and they both have constant dielectric permittivity, the wave speed through the composite can be fully determined through **Eq. (7)**.

$$v_{w,sensor} = \frac{c}{n} = \frac{c}{\sqrt{\varepsilon_r \, \mu_r}} \approx \frac{c}{\sqrt{\varepsilon_{r,eff}}} \quad \textbf{(7)}$$

Since the particles are several order of magnitudes smaller than the wavelength of a THz wave, the sensor can be considered homogeneous for electromagnetic processes and $\varepsilon_{r,eff}$ will be a combination of the dielectric permittivity of both constituents that will depend on the particle density of the particle composite, as it is stated by the Lichtenecker rule [47] in **Eq. (8)**, where ε_p, ε_m are the dielectric constants of the particles and matrix respectively, b is a fitting constant and v_r is the volumetric ratio of particles to matrix.

$$\log\left(\varepsilon_{r,eff}\right) = \log\left(\varepsilon_p\right) + v_r \cdot (1 - b) \cdot \log\left(\frac{\varepsilon_m}{\varepsilon_p}\right) \quad \textbf{(8)}$$

In conclusion, the important information to apprehend from this subsection is that the ToA measured at each load will be determined by the thickness of the sensor t_{sensor} and the dielectric permittivity of the composite $\varepsilon_{r,eff}$. Since the former will determine how long is the wave traveling at the lower speed $v_{w,sensor}$ instead of the faster $v_{w,air}$, and the latter will determine the magnitude of $v_{w,sensor}$. Then, these magnitudes will change with strain, changing the time of arrival and allowing to sense it, the next subsections focus on explaining how these two factors will change with volumetric strain, proving that it is what we are actually sensing instead of other phenomena, and proposing mathematical relations to analytically calculate ΔToA for an applied e_{vol}.

3.2.3 Change in thickness effect

As already explained, applying an in-plane strain to the sensor will produce a change in thickness through the Poisson's effect, which will change how long is the THz wave experiencing a slower phase velocity $v_{w,sensor}$, influencing the ToA. This change in thickness can be easily quantified if a constant Poisson's ratio and hyper-elasticity are assumed. Theoretically, Poisson's ratio dependance with stress could be calculated, but it requires intricate thickness measurements, and it is not really needed for the purpose of this theoretical model. With regard to hyper-elasticity, we are using PDMS as a matrix, which is an elastomer, and although cohesive failure with the particle may make it lose some of its high elastic properties, it should still be enough to carry out the assumption for the low strains applied in this process.

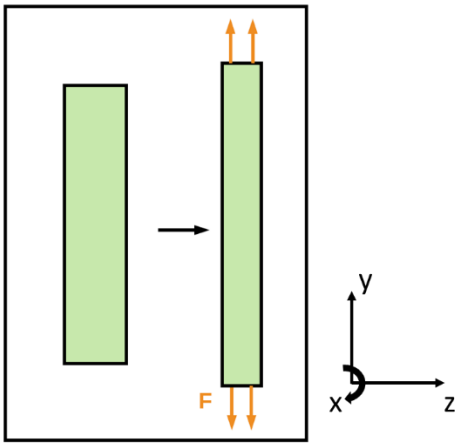

Figure 12: Change in thickness of sensor due to planar strain schematic. It also shows how the reference frame used for the analysis.

Change in thickness t with strain can be related to transversal strain e_{zz} through **Eq. (9)**, the directions of strain can be understood through **Figure 12**. Also, note strain will be expressed with the letter e to avoid confusion with dielectric constant ε. Following up, by means of hyper-elasticity, 2D volumetric strain can be expressed for small strains with **Eq. (10)**, where the product

is usually neglected for small strains. Then, volumetric is related to transversal strain through Poisson's ratio as seen in **Eq. (11)**, which can be used to obtain an analytical expression relating Δt with e_{vol}.

$$\Delta ToA\ \alpha\ t, \qquad t_f = t_o * (1 + e_{zz}) \tag{9}$$

$$e_{vol} = e_{xx} + e_{yy} + e_{xx}e_{yy} \approx e_{xx} + e_{yy} \tag{10}$$

$$e_{zz} = -\frac{v}{1-v} \cdot \left(e_{xx} + e_{yy}\right) = -\frac{v}{1-v} \cdot e_{vol} \tag{11}$$

$$t_f = t_o \left(1 - \frac{v}{1-v} \cdot e_{vol}\right) \tag{12}$$

$$\Delta ToA \propto \frac{1}{e_{vol}} \tag{13}$$

This analysis yields a direct proportionality between ΔToA and e_{vol} , expressed by α in **Eq. (13)**, therefore agreeing with our initial statement that applying planar strain will decrease thickness and produce a change in ΔToA, and also obtaining an expression to calculate it. Introducing **Eq. (12)** in the sensor thickness of **Eq. (4)**, it is possible to calculate what effect will have the change in thickness on ΔToA without any other effects being considered. This is displayed in **Figure 14** in the next section comparing to the effect induced by dielectrostriction.

3.2.4 Change in particle density effect

An expression for the change in dielectric permittivity with strain, also called dielectrostriction, of a dispersed particles composite has already been developed by Ref. [48]. Conveniently, it yields a function of measurable properties and principal strains ($e_{\xi\xi}$), allowing to easily calculate it. The expression is displayed in **Eq. (14)**, and it is a function of the permittivity

of the undeformed composite ε^i, the permittivity of the polymer matrix ε_m, and permittivity of vacuum ε^0; which are quantities measurable for THz frequencies with the same set up used for this work. This is accomplished by a similar kinematic quantification of the difference between a wave passing through air. Using this method, the values obtained where $\varepsilon_m \cong 2.95$, and $\varepsilon^i \cong 5.1$ for the sensor with 8% of particles in volume used in the experiments.

$$\varepsilon_{\xi\xi} = \varepsilon^0 + a_1 \cdot e_{\xi\xi} + a_2 \cdot e_{kk}$$

$$a_1 = -\frac{2}{5}\,\frac{\left(\varepsilon^i - \varepsilon_m\right)^2}{\varepsilon_m} \qquad \textbf{(14)}$$

$$a_2 = -\frac{1}{3}\,\frac{\left(\varepsilon^i - \varepsilon_m\right)\left(\varepsilon^i + 2\varepsilon_m\right)}{\varepsilon_m} + \frac{2}{15}\frac{\left(\varepsilon^i - \varepsilon_m\right)^2}{\varepsilon_m}$$

As it can be seen, these equations states that there will be different components of dielectric permittivity, and that those will be aligned with the principal directions of strain that is being experienced by the material. This conflicts with our initial assumption that the material would have rotational symmetry in its permittivity, since it shows that strain would produce dielectric anisotropy, so an electromagnetic wave will have different speeds along the material depending on its polarization. However, we are using a non-polarized wave; this kind of waves are hard to model accurately, since the wave is changing its polarization state randomly and in an almost instant manner. To model this, they are usually assumed to have half its oscillations in two perpendicular directions, which is represented in **Figure 13**. These directions can be set arbitrarily as long as they are perpendicular, so they can be aligned with the principal directions of strain, which are also perpendicular.

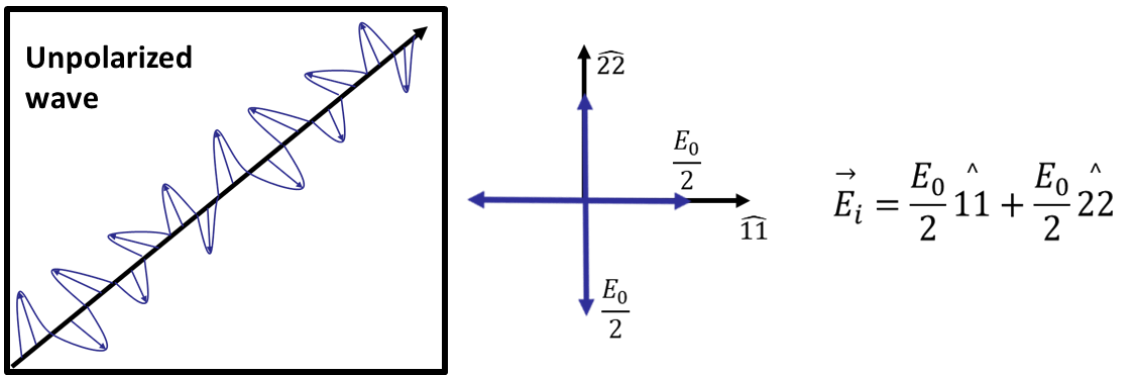

Figure 13: Mathematical modeling of unpolarized wave propagating in direction 33. They are assumed to have half of its oscillations in the two planar perpendicular directions.

This yields the opportunity to produce an equation for an effective dielectric permittivity in terms of 2D volumetric strain that we can use with our previous equations, which will be an average between dielectric permittivity in the two directions of principal strain, ε_{11} and ε_{22}, expressed in **Eq. (15)**.

$$\varepsilon_{eff} = \frac{(\varepsilon_{11} + \varepsilon_{22})}{2}$$

$$\begin{cases} \varepsilon_{11} = \varepsilon^i + a_1 \cdot e_{11} + a_2 \cdot (e_{11} + e_{22} + e_{33}) \\ \varepsilon_{22} = \varepsilon^i + a_1 \cdot e_{22} + a_2 \cdot (e_{11} + e_{22} + e_{33}) \end{cases} \quad \textbf{(15)}$$

$$\varepsilon_{eff} = \varepsilon^i + a_1 \cdot \frac{e_{vol}}{2} + a_2 \cdot \left(e_{vol} \left(1 - \frac{v}{1-v} \right) \right)$$

$$\varepsilon_{eff} = \varepsilon^i + e_{vol} \cdot \left(\frac{a_1}{2} + a_2 \cdot (1 - \frac{v}{1-v}) \right)$$

From this expression, an equation that proposes a direct relation between 2D volumetric strain and the dielectrostriction of our composite has been yielded. Furthermore, it also shows a linear relation, which is in accordance with our experimental results. This is discussed

with further detail in the comparison between the analytical and experimental results. Since we quantified the influence on ΔToA, now it is possible to proceed with **Eq. (4)** to compare with the effect produced by a change in thickness. This is displayed in **Figure 14**, and it shows than the Poisson's effect is slightly more dominant than the electrostriction for our sensor, but both have a similar effect in the ΔToA,

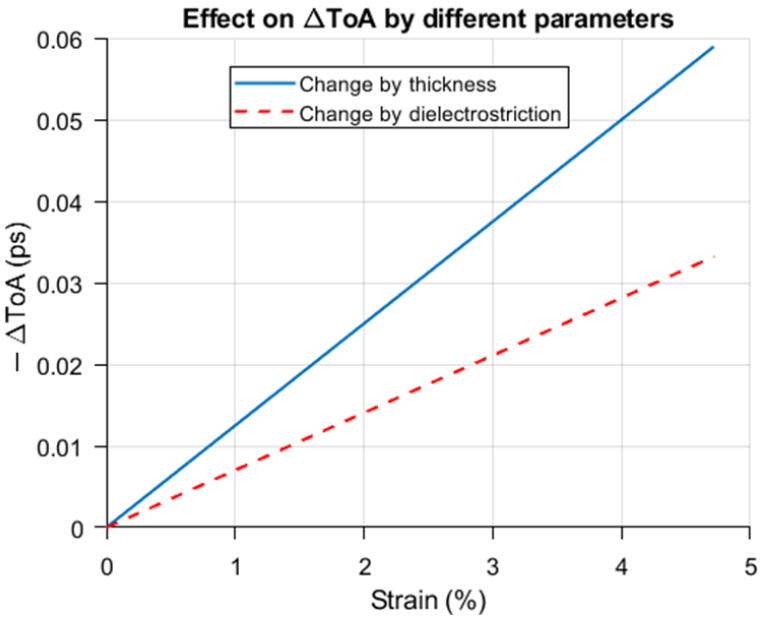

Figure 14: Effect on ΔToA by dielectrostriction and change in thickness. It shows they have a similar influence on the sensor sensitivity, with the change in thickness being slightly larger.

3.2.5 Stress on STO filler effect

Strontium Titanate's dielectric sensitivity to stress has been extensively studied [49], [50], [51]. According to Ref. [49], the dielectric constant of STO single crystal decreases with compressive pressure, and Ref. [52] states that it also decreases with tensile stress. This means that any stress state will decrease the dielectric constant of the filler in our composite; this would increase the sensitivity in the case of tension, since it will be another factor in decreasing the ToA

with strain, but on the other hand it will decrease sensitivity for compressive strain measurements, since it will decrease ToA while the other factors are increasing it. However, the order of magnitude of stress in STO needed to produce a significant amount of change in its dielectric for us to measure is too high to achieve on a particle filler inside an elastomer. The order of magnitude of the stress that the particle filler is experiencing can be calculated under certain assumptions, a schematic is shown in **Figure 15**.

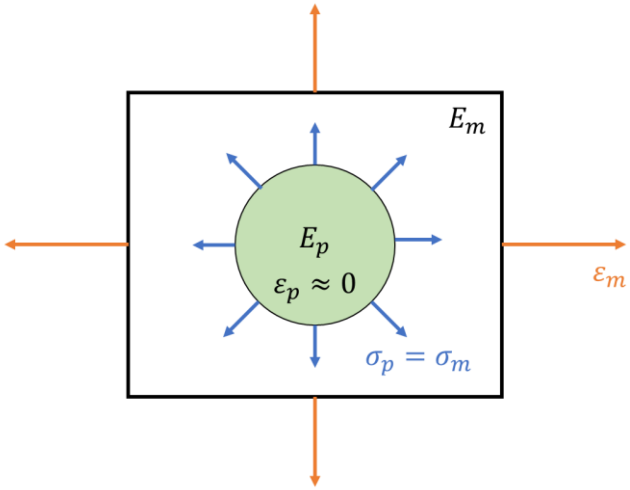

Figure 15: Schematic of stress produced on STO filler particle by deformation of the elastomer matrix.

Since the elastic constant of the ceramic particle is much larger than the elastomer matrix ($Ep >> Em$), we can assume that the STO particle is not deforming ($\varepsilon_p \approx 0$). This way, all the strain that we are measuring or applying will be produced in the matrix and not in the particle. Then, by assuming a fully bonded boundary condition at the surface between the particle and the elastomer, we can obtain the stress in the particle, which we can calculate through elasticity and superposition, as shown in **Eq. (16)** for the stress experienced around a rigid circular inclusion in uniaxial strain.

$$\sigma_p = \sigma_{yy} * \frac{5 + v_1}{3 + 2v_1 - {v_1}^2} = \varepsilon_m \cdot E_m * \frac{5 + v_1}{3 + 2v_1 - {v_1}^2} \quad \textbf{(16)}$$

For the highest strain value that has been measured in the experiments, which is of the order of $\varepsilon_m = 0.1$, and using a young modulus for PDMS of $E_m = 1Mpa$ and a Poisson's ratio of $v = 0.5$ [53], a particle stress of $\sigma_p = 0.147\ Mpa$ is reported on the STO particle. According to the experimental data from Ref. [11], that would produce a change in dielectric constant of the STO of 0.03%, which can be considered negligible.

In conclusion, the effect on dielectrostriction of the composite by the dielectrostriction of the STO filler itself due to stress will not be affecting the sensitivity of our method in a significant matter, so it can be eliminated from the discussion. Also, this model also does not account for cohesive failure, where the polymer and particle bonding breaks and the particle will not be stressed anymore, which is probably happening and will decrease this effect even more.

3.2.6 Results of Theoretical Model and Comparison with Experimental Results of ΔToA

Once all the influences on ΔToA have been discussed and modeled, it is possible to calculate the overall change in ToA with strain for a certain dispersed particle composite that accomplishes they taken assumptions. All the data needed are its initial thickness t, its Poisson's ratio v, the dielectric permittivity of the matrix ε_m and the dielectric permittivity of the undeformed composite ε^i. For the sensor prototype developed in this thesis, its thickness was $t = 0.5\ mm$ and the Poisson's ratio was $v = 0.4$, which is smaller than PDMS [54] due to the stiff particles inside. The dielectric permittivities used for the model were obtained by measuring the time-delay with respect to air in a THz wave going through a slab of the material with known thickness, and using similar kinematic equations to the described here, a dielectric permittivity of $\varepsilon^i = 5.1$ for the composite

of this study and $\varepsilon_m = 2.95$ for PDMS were obtained. This is a usual method to measure dielectric permittivity at THz frequency of materials. The analytical results obtained are plotted in **Figure 16** and compared with the results obtained through experiments in a tensile test with known applied strain.

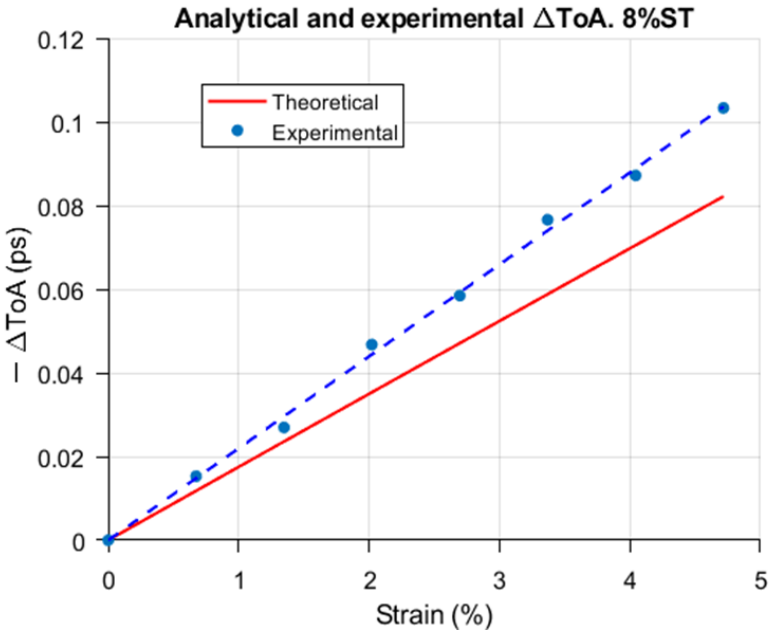

Figure 16: Experimental and analytical results of ΔToA with strain.

The theoretical results show a slightly higher sensitivity to strain than the experiments, but both have very similar magnitude and produce a linear response. This can be taken as an indication that we are indeed sensing the physical phenomena described, that the model produced is accurate, and that composites made with these characteristics can be used for volumetric contactless strain sensing through THz TDS probing by previous linear calibration.

3.3 Experimental Procedures

3.3.1 Sample Preparation and Design

The composite sensor prototype for this report has been prepared in lab by dispersion into PDMS resin of strontium titanate particles with size below 5 μm purchased from Sigma Aldrich, mixed, and then hardener was added to the mixture. PDMS was chosen as an elastomer matrix due to its high elasticity, ease of preparation and curing and good flow properties. The proportions where chosen to obtain a composite with 8% STO in volume; this was found optimal since even a higher number of particles increased the sensitivity of the composite, it made it too viscous, which increased the imperfections such as air bubbles and particle conglomerations. This could probably be fixed with better manufacturing methods that were not available to us at the time. Afterwards, the still viscous mixture was introduced in a 3D printed container as shown in **Figure 17** with a height of 0.5mm, which will yield the thickness of the coating; this thickness was chosen in order to have a coating that maximizes its impact on the spectral measurements but thin enough that it still satisfied plane stress condition and that the strain at one side of the plane would be the same as the other, so it is accurate if used as a strain gauge. To reduce the amount of air bubbles and imperfections in the matrix, the composite was introduced in a vacuum chamber during curing. This should produce an isotropic composite due to the small size of the particles and their random distribution that was also elastic enough not to interfere with the structural behavior of the component to which it will be attached to. The samples were then shaped into the desired geometries through punching methods, which had higher accuracy than modeling.

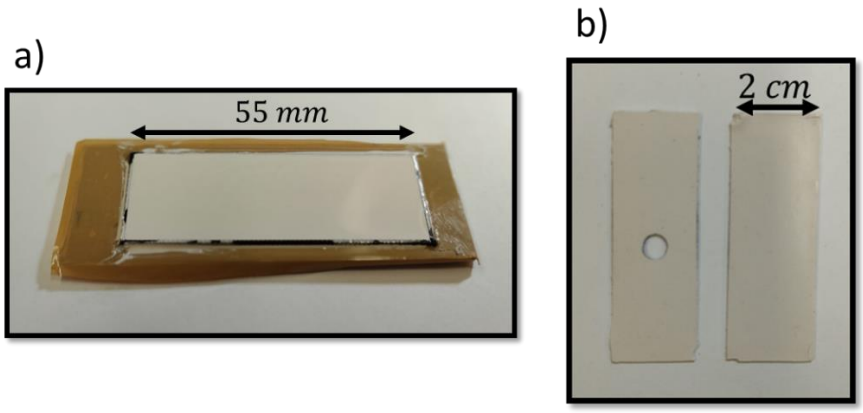

Figure 17: Picture of fully cured composites of STO particles dispersed in PDMS. **a)** shows the composite inside the mold once it is fully cured. **b)** shows different composites once they have been detached, it also shows a sample that has been punched to produce a circular hole for strain gradient mapping

3.3.2 Experimental Set-Up

THz measurements have been performed using a BATOP TDS-1008 with fiber coupled antennas that allowed for proper positioning of the THz wave and scanning of multiple points, which made possible to obtain accurate THz imaging and therefore to produce contours of the measured strains at the different points through the sample. The distance between the antennas was 60 mm as specified by the manufacturer when using the focusing lenses, which allowed for a beam resolution of 0.4mm when positioning the sample at 30 mm from each antenna where the focusing of the THz waves is at its maximum.

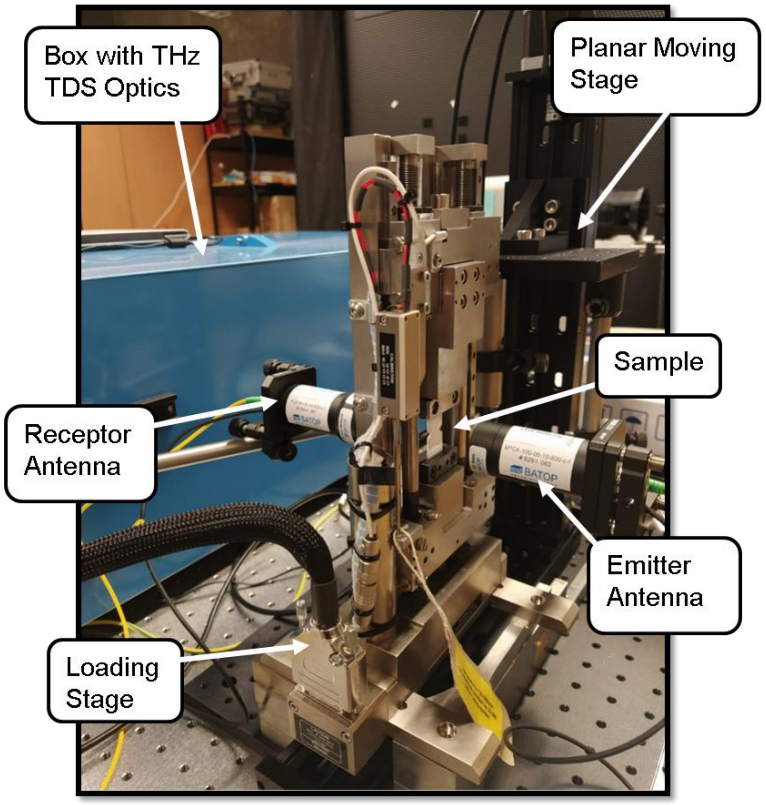

Figure 18: Picture of experimental set up showing loading stage with notched sample and THz spectrometer with fiber-coupled antennas.

To apply tensile loads to the coated samples, a Microtest 2kN loading stage was needed to fit it in the THz TDS set up, which allows to specify accurate extensions, loadings and strain rates; the specimen to be tested were clamped onto the loading stage through dented metal clamps. The set-up is shown in **Figure 18**.

3.3.3 DIC Measurements

To check the strain measurements produced through THz TDS they have been compared with Digital Image Correlation (DIC) measurements. The images for DIC were taken on the same samples but after the THz measurements were finished because the speckle patterns needed for DIC could affect the THz readings. Since the material is highly elastic it could be unloaded and

loaded within certain limits without its behavior changing significantly. The speckle pattern used was black paint spray and it was applied without removing the sample from the loading stage to avoid changing the gripping state of the sample, it can be seen in **Figure 19**. The DIC analysis of the images was performed using the software VIC-2D, and a function was applied to obtain volumetric strain from the default strain outputs.

Figure 19: Picture of sample with applied spackle pattern through black spray paint to be used for DIC.

3.3.4 FEA Simulations

FEA simulations were produced using Abaqus CAE as another method of comparison with the strain measurements. They consisted of hyperplastic simulations with planar stress state, with the sample dimensions and gripping area as the experiments. Only displacements were applied, and since the only output needed from the program was strain, no exact materials properties were needed and the elasticity constant of PDMS could applied. To obtain volumetric strain, it needed to be created as a new field output, which did not allow to show the deformed shape and the volumetric strain field output at the same time. Element convergence studies were performed.

3.3.5 Data Acquisition and Analysis

THz TDS yields the amplitude behavior in time of the received THz EMP in time with high accuracy, which makes possible to calculate small changes in the media through which the pulse goes through, as can be seen in **Figure 20**. This plot shows the THz spectra of two waves that have traveled through the same material with different uniaxial loadings, as it can be seen there is a change in amplitude and phase. The changes in amplitude are not as reliable to measure strain because the equipment is not able to produce the exact same amplitude in every measurement due to instabilities. Nonetheless, it can keep a constant emission time with high accuracy, so the phase change can be used to sense the small change produced by strain measurements. As explained in the theoretical model, amplitude and velocity of the wave through dielectric media are unrelated, so instabilities in amplitude will not produce instabilities in phase.

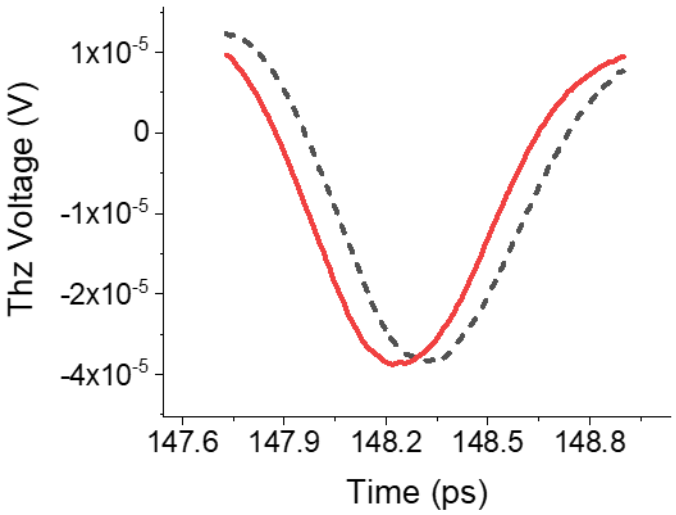

Figure 20: THz Time Domain Spectra of electro strictive coating for a loaded and unloaded case, showing a change in phase.

In order to best calculate the change in TOA of the wave, the most optimal way found for the big amount of data required to analyze for a full strain mapping was to calculate the phase-delay using

a simplification where the phase change is quantified as the angle between two vectors and obtained using the dot product. It consists of using Error! Reference source not found. by treating t he sampled amplitude for the waves measured at the same times as two vectors, and then calculating the angle that would be formed between these vectors as the dot product. This seems to yield a very effective and computationally cheap way to find the difference produced between the waves that go through the loaded and unloaded composite. This expression will yield ϕ, is the phase difference between the unloaded and loaded wave results; $\vec{a}$ and $\vec{b}$ will be the sampled amplitude of the unloaded and loaded wave data expressed as vectors, respectively.

.

$$\vec{a} \cdot \vec{b} = \left|\vec{a}\right| \cdot \left|\vec{b}\right| * \cos(\phi) \rightarrow \cos(\phi) = \frac{\vec{a} \cdot \vec{b}}{\left|\vec{a}\right| \cdot \left|\vec{b}\right|} \qquad \textbf{(17)}$$

This method is the one that is used for the strain mappings since it significantly reduced the computation time to analyze the big data in the mappings. Another method possible to measure phase-delay is to find the position in time of the peak in the THz spectra obtained, which also yielded a reliable sensitivity to strain, this is the method that has been used to calculate ΔToA for comparison with the theoretical model since it allowed to directly sense changes in time, which is what the model yields. This was performed by a Fourier peak fitting of the THz signal. A comparison between the data obtained between both data analysis methods is displayed in **Figure 21**. As it can be seen, they both show a very similar behavior, so the phase-delay calculation explained is viable to use as a measurement method to save computing time.

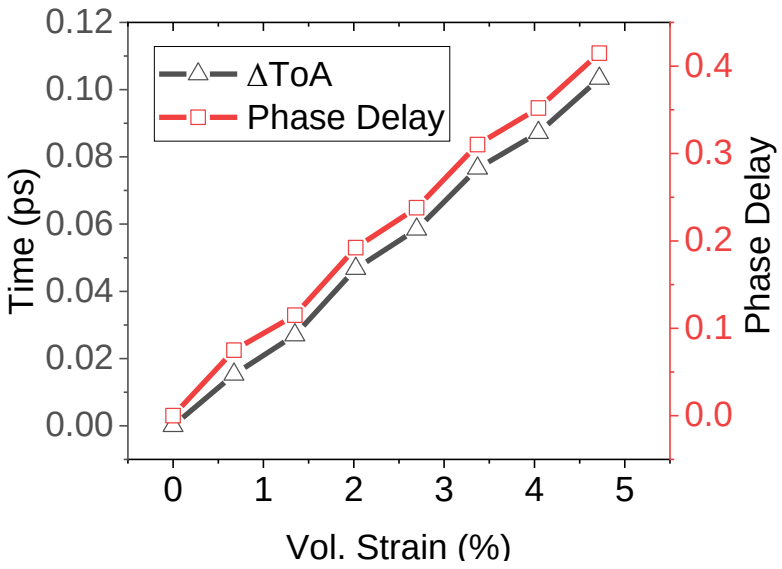

Figure 21: Effect of Volumetric on THz spectra measurements showing how it affects a change in peak position and a phase-delay. Both show a very similar behavior.

The method used for the measurements of strain maps is to produce THz TDS along different points of a surface by moving the emitter and receptor antenna simultaneously in the direction perpendicular area of mapping. This way, it is possible to obtain the same data as **Figure 21** for each measured point along the mapped surface for different loadings, and using the calibration a value of strain can be assigned to each point and a contour can be obtained. The spatial resolution of a usual THz TDS system with focusing lenses is around 0.4mm, which will limit the pixel size of the contour.

3.4 Results and Discussion

3.4.1 Material Specific Calibration

Firstly, a composite was manufactured with the shape of a tensile test specimen and strained with a loading stage to calculate the change of ΔToA for a known applied volumetric strain. These results are shown in **Figure 21** in the previous section, where a linear behavior can be seen. This proves that the sensor is working with the characteristics previously predicted in the theoretical background. This data was then used as calibration to measure strain in the same material and thickness but for other specimens with unknown geometrical characteristics using **Eq. (18)**, where C will be the slope of the linear data obtained in the calibration and ϕ the phase difference between the waves measured for the loaded and unloaded specimen. For the STO in PDMS prototype produced and studied in this work, the calibration yielded a slope $C = 0.0869$ for calculating strain through a phase-delay.

$$e_{vol} = C \cdot \phi \qquad \textbf{(18)}$$

3.4.2 Strain Imaging

The following figures show the different strain maps obtained with this method and how they compare to FEA simulations and DIC measurements. Three different geometries were studied: a circular edge-notch, a center circular hole, and an edge crack. For each geometry, three different loads were applied, where the applied vertical strain is symbolized in the figures as ε_{yy}.

The first contours shown in **Figure 22** are results that show the strain imaging plotted applying the same limits to the contour colorbars to show that there is some error in the upper limits of THz compared to the other methods. Afterwards, the plots will have the same limits, to show that the

method is reliable in capturing strain distributions even though the upper and lower limits may not be fully accurate. This could be explained by instabilities in the measurement equipment that grow with time of between measurements.

3.4.3 Strain measurement example with same contour limits

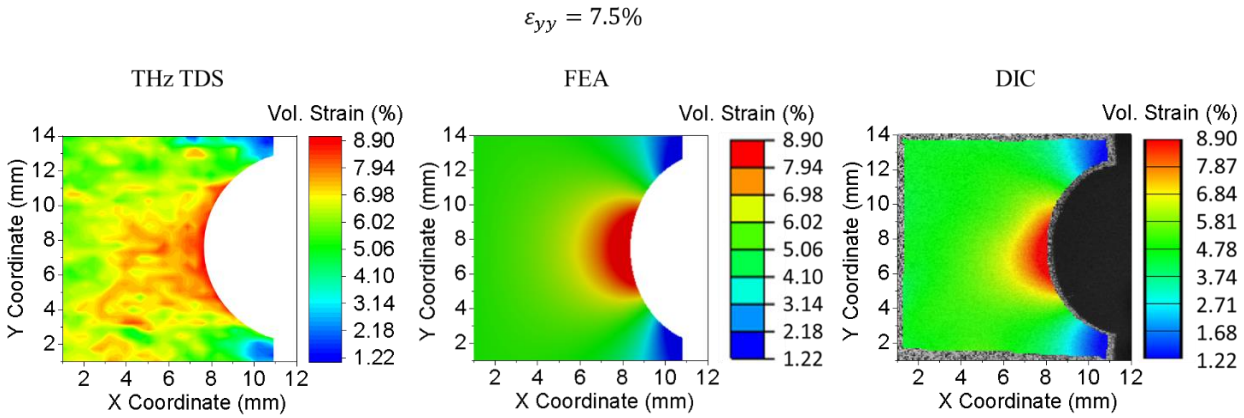

Figure 22: Volumetric strain measurements for the circular edge-notch specimen for an axial applied strain of 7.5% with the same limits for the contour value, showing that there is some error in the THz-TDS measurements. However, in the rest of the results it can be appreciated that this technique is still useful to obtain the strain distribution although the limits may not be fully accurate.

3.4.4 Circular Edge-Notch Strain Measurements

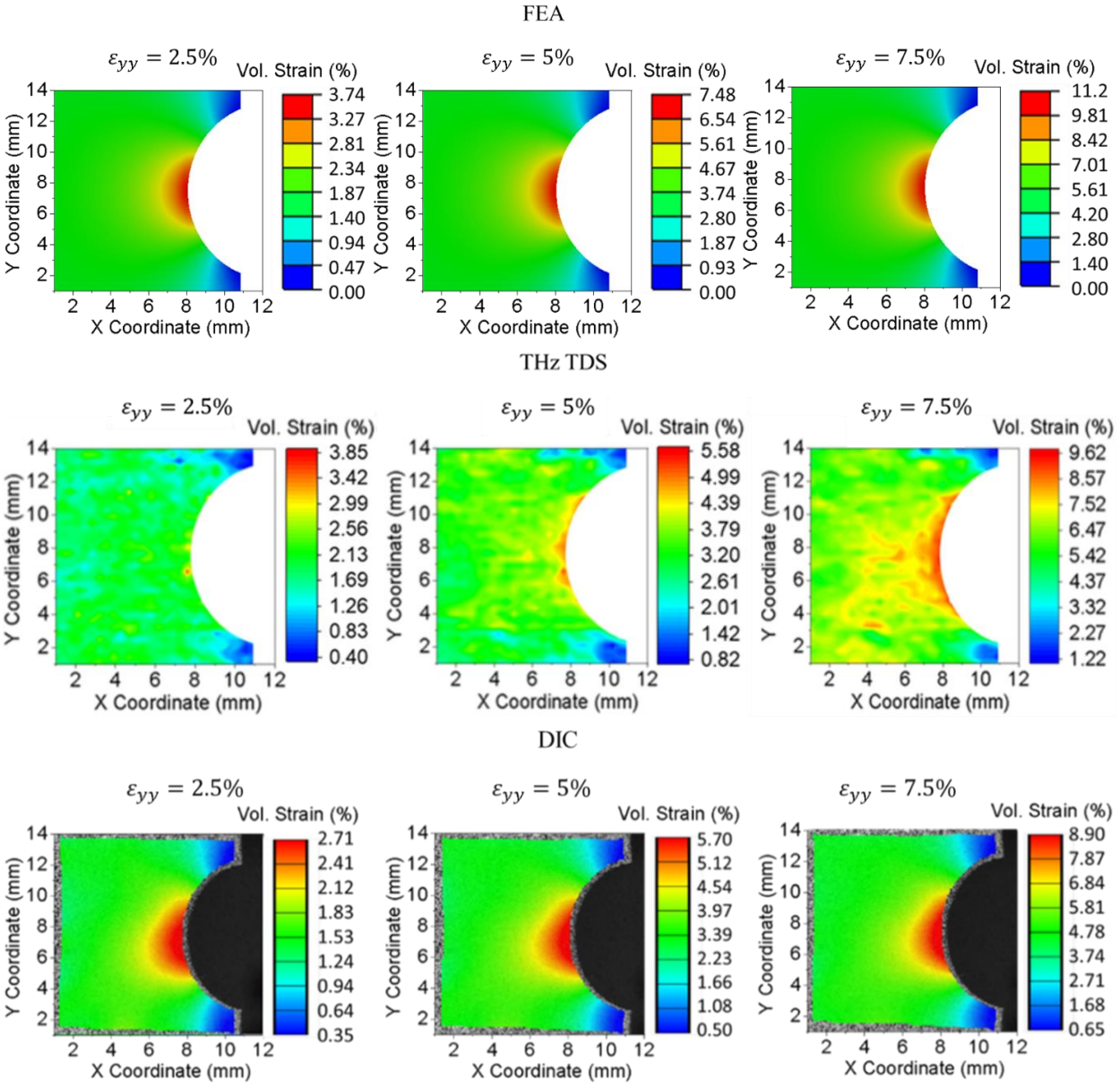

Figure 23: Circular edge-notch Strain Measurements.

3.4.5 Edge Crack Strain Measurements

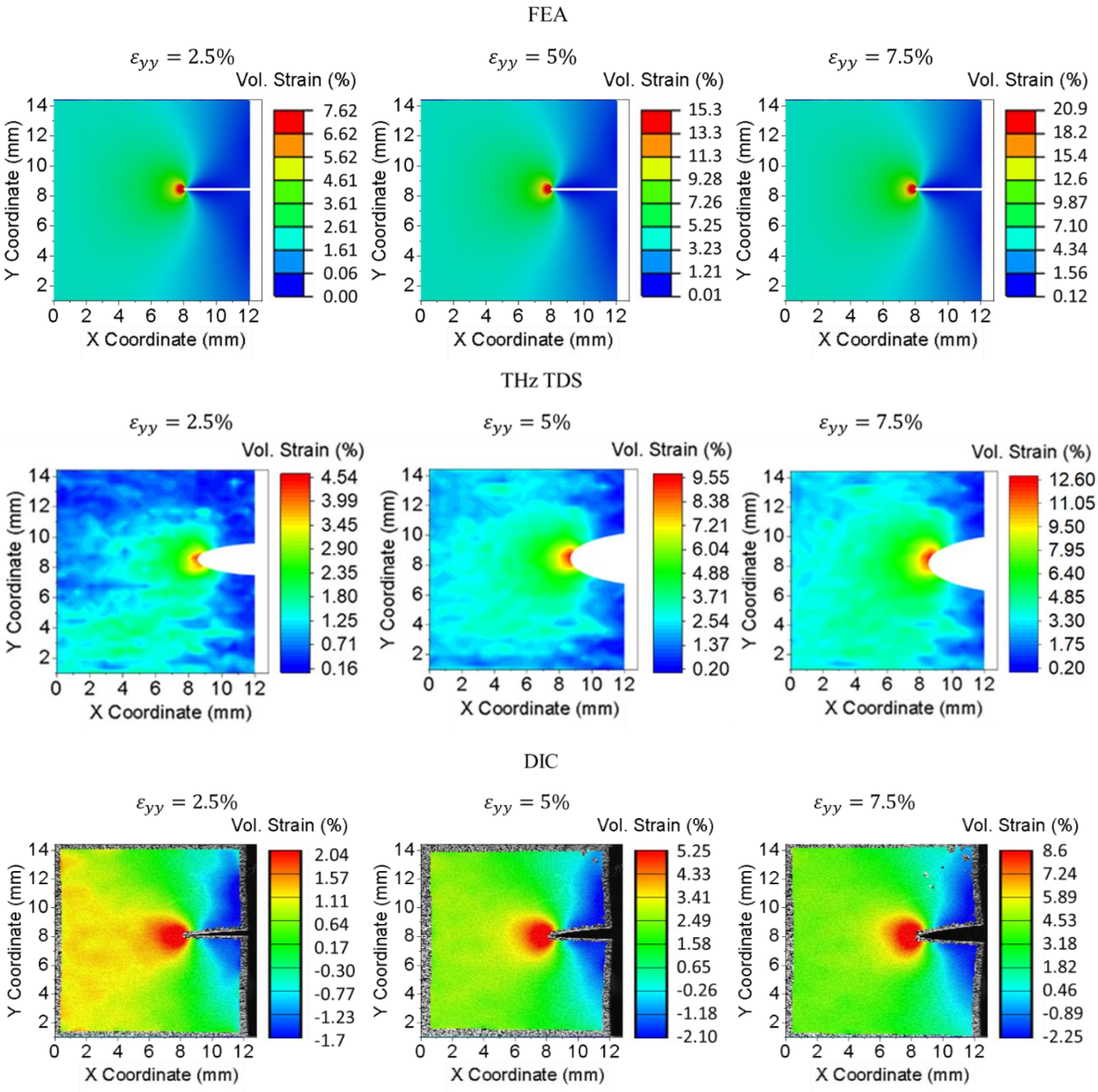

Figure 24: Edge-crack Strain Measurements.

3.4.6 Circular Hole Strain Measurements

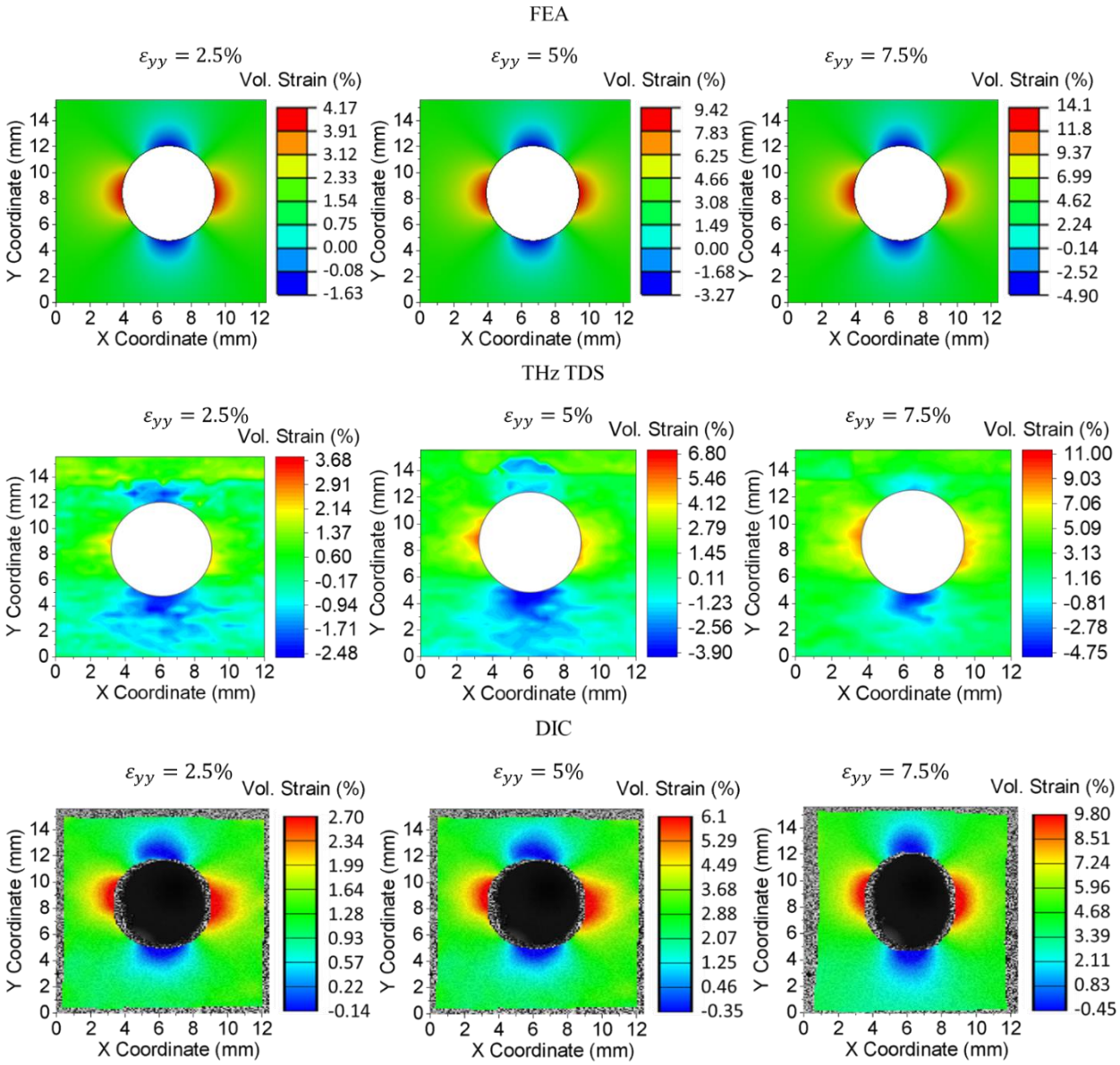

Figure 25: Circular hole Strain Measurements.

From these results, it can be seen that measurements through THz TDS are able to sense and map strain gradients through probing the developed sensor. The values THz TDS obtained for most of the results in the range between the values yielded by FEA and DIC; this can be due to DIC not being able to measure the regions where the displacement is too large, which is where the strain is larger and therefore sets the limits of the contour. However, the sensitivity obtained is not as high as DIC and the contours do not look as smooth or THz TDS, so efforts are still needed to provide the higher sensitivity if this method is to be used for a wider range of applications. One idea would be to increase the volumetric ratio of particles while producing also improving manufacturing, so air bubbles and particle conglomerations are avoided. This would not only increase dielectrostriction, but it would also increase the overall dielectric constant of the composite so the change in thickness effect on the phase-delay would also be increased. It is also important to note that if this sensor is to be used for measure of strain in metal surfaces through a reflection configuration, the wave will travel twice through the sensor, which should produce higher values of ΔToA and increase sensitivity.

CHAPTER 4. CONCLUSIONS

Development of a composite that changes its dielectric constant with stress has been carried out with the objective of producing a new method of structural health monitoring through remote sensing by THz TDS, where the composite will be used as a coating that performs as a passive sensor. By measuring the change in time of arrival of a THz wave that goes through it when it is loaded, localized changes in strain can be quantified.

To prove the functionality of the sensor; firstly, a theoretical model has been developed of the physics that will affect the THz TDS spectra obtained. This model quantified the effect on the measured ToA by different characteristics of the composite changing with volumetric strain, being the main ones a change in thickness and dielectrostriction through particles dispersion. Both effects decreased ToA linearly with tensile strain and decreased it with compressive, so they can be used for volumetric strain measurements through previous material specific calibration.

Then, a composite prototype has been produced and the change of arrival has been measured for different loads, showing a linear behavior with a similar magnitude to the results from the theoretical model, showing that we are sensing the effects studied in the theory.

Finally, these results were used as a calibration to measure the map strain in several samples of the same material with different geometries, showing the ability to produce strain images of small regions by the application of this technique along several points of a surface to produce a contour. This method still has some error that could be reduced by increasing the volumetric ratio of STO, this will be attended in future work together with surface strain measurement of metals through sensor attachment and a reflection configuration

REFERENCES

1. Neu, J. and C.A. Schmuttenmaer, *Tutorial: An introduction to terahertz time domain spectroscopy (THz-TDS).* Journal of Applied Physics, 2018. **124**(23): p. 231101.

2. Jepsen, P.U., D.G. Cooke, and M. Koch, *Terahertz spectroscopy and imaging – Modern techniques and applications.* Laser & Photonics Reviews, 2011. **5**(1): p. 124-166.

3. Wang, Y., et al., *Terahertz absorbance spectrum fitting method for quantitative detection of concealed contraband.* Journal of Applied Physics, 2007. **102**(11): p. 113108.

4. Danciu, M., et al. *Terahertz Spectroscopy and Imaging: A Cutting-Edge Method for Diagnosing Digestive Cancers*. Materials (Basel, Switzerland), 2019. **12**, DOI: 10.3390/ma12091519.

5. Lloyd-Hughes, J. and T.-I. Jeon, *A Review of the Terahertz Conductivity of Bulk and Nano-Materials.* Journal of Infrared, Millimeter, and Terahertz Waves, 2012. **33**(9): p. 871-925.

6. Li, J. and K. Chang, *Electric field driven quantum phase transition between band insulator and topological insulator.* Applied Physics Letters, 2009. **95**(22): p. 222110.

7. Zhao, J., et al., *Terahertz imaging with sub-wavelength resolution by femtosecond laser filament in air.* Scientific Reports, 2014. **4**(1): p. 3880.

8. Choudhury, D., et al., *Tuning of dielectric properties and magnetism of SrTiO${}_{3}$ by site-specific doping of Mn.* Physical Review B, 2011. **84**(12): p. 125124.

9. Zamudio-Lara, A., et al., *Frequency multiplication of terahertz radiation in the crystals of strontium titanate paraelectric.* Radioelectronics and Communications Systems, 2015. **58**(9): p. 411-416.

10. Dhiman, A., et al., *Strontium Titanate Composites for Microwave-Based Stress Sensing*. JOM, 2018. **70**(9): p. 1811-1815.

11. Samara, G.A. and A.A. Giardini, *Pressure Dependence of the Dielectric Constant of Strontium Titanate.* Physical Review, 1965. **140**(3A): p. A954-A957.

12. Shaw, T.M., et al., *The effect of stress on the dielectric properties of barium strontium titanate thin films.* Applied Physics Letters, 1999. **75**(14): p. 2129-2131.

13. Aubert, T., O. Elmazria, and M.B. Assouar. *Wireless and batteryless surface acoustic wave sensors for high temperature environments*. in *2009 9th International Conference on Electronic Measurement & Instruments*. 2009.

14. Dai, X., et al., *Design of a Novel Passive Wireless Integrated SAW-Based Antenna Sensor for Structural Health Monitoring.* Journal of Sensors, 2020. **2020**: p. 6121907.

15. Wilson, W.C. and G.M. Atkinson, *Surface Acoustic Wave Strain Sensor Model.* Sensors and Transducers, 2011. **11**: p. 23-33.

16. Xin, G., et al., *Distributed sensing technology of high-spatial resolution based on dense ultra-short FBG array with large multiplexing capacity.* Optics Express, 2017. **25**(23): p. 28112-28122.

17. Li, J., et al., *High spatial resolution distributed fiber strain sensor based on phase-OFDR.* Opt Express, 2017. **25**(22): p. 27913-27922.

18. Jeong, H. and S. Lim, *A Stretchable Radio-Frequency Strain Sensor Using Screen Printing Technology.* Sensors, 2016. **16**(11): p. 1839.

19. Occhiuzzi, C., C. Paggi, and G. Marrocco, *Passive RFID Strain-Sensor Based on Meander-Line Antennas.* IEEE Transactions on Antennas and Propagation, 2011. **59**(12): p. 4836-4840.

20. Tahara, T., et al., *Digital holography and its multidimensional imaging applications: a review.* Microscopy, 2018. **67**(2): p. 55-67.

21. Wang, Y.Y. and J. Bruley, *Dual Lens Electron Holography for High Spatial Resolution Junction and Strain Mapping of Semiconductor Devices.* Microscopy and Microanalysis, 2014. **20**(S3): p. 240-241.

22. Denneulin, T., F. Houdellier, and M. Hÿtch, *Differential phase-contrast dark-field electron holography for strain mapping.* Ultramicroscopy, 2016. **160**: p. 98-109.

23. Wang, Q., H. Tsuda, and H. Xie, *Developments and Applications of Moire Techniques for Deformation Measurement, Structure Characterization and Shape Analysis.* Recent Patents on Materials Science, 2015. **08**: p. 1-1.

24. Chen, B. and C. Basaran, *Measuring Joule heating and strain induced by electrical current with Moiré interferometry.* Journal of Applied Physics, 2011. **109**(7): p. 074908.

25. Chen, B. and C. Basaran, *Statistical phase-shifting step estimation algorithm based on the continuous wavelet transform for high-resolution interferometry metrology.* Applied Optics, 2011. **50**(4): p. 586-593.

26. Paris, R., M. Melik-Merkumians, and G. Schitter, *Probabilistic Absolute Position Sensor Based on Objective Laser Speckles.* IEEE Transactions on Instrumentation and Measurement, 2016. **65**(5): p. 1188-1196.

27. Feiel, R. and P. Wilksch, *High-resolution laser speckle correlation for displacement and strain measurement.* Applied Optics, 2000. **39**(1): p. 54-60.

28. Roncella, R., et al., *Comparative Analysis of Digital Image Correlation Techniques for In-plane Displacement Measurements*. 2012.

29. Słoński, M. and M. Tekieli, *2D Digital Image Correlation and Region-Based Convolutional Neural Network in Monitoring and Evaluation of Surface Cracks in Concrete Structural Elements.* Materials (Basel, Switzerland), 2020. **13**(16): p. 3527.

30. Mao, L., et al., *3D Strain Mapping of Opaque Materials Using an Improved Digital Volumetric Speckle Photography Technique with X-Ray Microtomography.* Applied Sciences, 2019. **9**: p. 1418.

31. Piombini, H., et al., *Stress measurement of elastic sol-gel layer by photoelasticimetry - comparison with Stoney.* Optical Materials Express, 2016. **6**(2): p. 469-485.

32. Wang, Z., et al., *Determination of plane stress state using terahertz time-domain spectroscopy.* Scientific Reports, 2016. **6**(1): p. 36308.

33. Knipe, K., et al., *Synchrotron X-Ray Diffraction Measurements Mapping Internal Strains of Thermal Barrier Coatings During Thermal Gradient Mechanical Fatigue Loading.* Journal of Engineering for Gas Turbines and Power, 2015. **137**(8).

34. Jakobsen, A.C., et al., *Mapping of individual dislocations with dark-field X-ray microscopy.* Journal of Applied Crystallography, 2019. **52**(1): p. 122-132.

35. Gan, M. and V. Tomar, *An in situ platform for the investigation of Raman shift in micro-scale silicon structures as a function of mechanical stress and temperature increase.* Review of Scientific Instruments, 2014. **85**(1): p. 013902.

36. Zhang, Y., C. Prakash, and V. Tomar. *In-situ Crack Tip Stress Measurement at High Temperature in IN-617 Using Combined Nano-Indentation and Nano-Mechanical Raman Spectroscopy*. in *Fracture, Fatigue, Failure and Damage Evolution, Volume 6*. 2019. Cham: Springer International Publishing.

37. Dhiman, A., et al., *Dynamic Stress Evaluation due to Hypervelocity Impact using Time Gated Raman Spectroscopy*. 2020.

38. Moriwaki, A., M. Okano, and S. Watanabe, *Internal triaxial strain imaging of visibly opaque black rubbers with terahertz polarization spectroscopy.* APL Photonics, 2017. **2**: p. 106101.

39. Okano, M. and S. Watanabe, *Internal Status of Visibly Opaque Black Rubbers Investigated by Terahertz Polarization Spectroscopy: Fundamentals and Applications.* Polymers, 2019. **11**(1).

40. Zhang, X. and Z. Liu, *Superlenses to overcome the diffraction limit.* Nature Materials, 2008. **7**(6): p. 435-441.

41. Landy, N.I., et al., *Perfect Metamaterial Absorber.* Physical Review Letters, 2008. **100**(20): p. 207402.

42. Schurig, D., et al., *Metamaterial Electromagnetic Cloak at Microwave Frequencies.* Science, 2006. **314**(5801): p. 977-980.

43. Melik, R., et al., *Metamaterial-Based Wireless Strain Sensors.* Applied Physics Letters, 2009. **95**: p. 011106-011106.

44. Li, J., et al. *Metamaterial-based strain sensors*. in *2011 Seventh International Conference on Intelligent Sensors, Sensor Networks and Information Processing*. 2011.

45. Everitt, H.O., et al., *Strain Sensing with Metamaterial Composites.* Advanced Optical Materials, 2019. **7**(9): p. 1801397.

46. Jang, S.-D., B.-W. Kang, and J. Kim, *Frequency selective surface based passive wireless sensor for structural health monitoring.* Smart Material Structures, 2013. **22**: p. 025002.

47. Hu, T., et al., *Dielectric properties of BST/polymer composite.* Journal of the European Ceramic Society, 2007. **27**(13): p. 3997-4001.

48. Shkel, Y.M. and D.J. Klingenberg, *Electrostriction of polarizable materials: Comparison of models with experimental data.* Journal of Applied Physics, 1998. **83**(1): p. 415-424.

49. Samara, G.A., *Pressure and Temperature Dependences of the Dielectric Properties of the Perovskites BaTi${\mathrm{O}}_{3}$ and SrTi${\mathrm{O}}_{3}$.* Physical Review, 1966. **151**(2): p. 378-386.

50. Silverman, B.D., *Microwave Absorption in Cubic Strontium Titanate.* Physical Review, 1962. **125**(6): p. 1921-1930.

51. Haeni, J.H., et al., *Room-temperature ferroelectricity in strained SrTiO3.* Nature, 2004. **430**(7001): p. 758-761.

52. Shaw, T., et al., *The Effect of Stress on the Dielectric Properties of Barium Strontium Titanate Thin Film.* Applied Physics Letters, 1999. **75**: p. 2129-2131.

53. Wang, Z., A.A. Volinsky, and N.D. Gallant, *Crosslinking effect on polydimethylsiloxane elastic modulus measured by custom-built compression instrument.* Journal of Applied Polymer Science, 2014. **131**(22).

54. Dogru, S., et al., *Poisson's ratio of PDMS thin films.* Polymer Testing, 2018. **69**: p. 375-384.